Dear Editor,

Please find below the point by point answers to the comments provided by both reviewers. In the following text, the comments of the reviewer are in written back and our answers are written in blue. All the modifications suggested by the reviewer have been carefully implemented into the manuscript. This updated version of the manuscript is available with the 'track changes' option at the end of this file, after our answers.

On behalf of all co-authors,
Goulven Laruelle

Review of bg-2017-64
Global high-resolution monthly pCO_2 climatology for the coastal ocean derived from neural network interpolation by Laruelle et al.
Reviewer: Rik Wanninkhof, NOAA/AOML
This is largely a descriptive paper of procedures to create monthly estimates of coastal pCO_2 levels. As mentioned in the abstract, Laruelle et al. use a modified version of a two-step artificial neural network method (SOM-FFN) to interpolate the pCO_2 data along the continental margins with a spatial resolution of 0.25 degrees and with monthly resolution from 1998 until 2014.
The effort is clearly an impressive one and an important contribution to coastal ocean science. However there are some shortcomings. Many readers will not fully understand the approach and assumptions in SOM-FNN. and this needs more discussion. The manuscript lacks in context and interpretation. Some of the procedural shortcomings that were in the initial global open ocean effort as described in Landschützer et al., (2013; 2015) prevail.

We are grateful for the reviewer's evaluation and his constructive suggestions. Please find bellow a detailed answer to each comment. All our answers are written in.
On behalf of all co-authors,

Goulven Laruelle

We have introduced a new section to the manuscript, which critically discusses the strength and weaknesses of the approach and its changes since the first open ocean version from Landschützer et al. (2013). This new section permits to better appraise the improvements achieved by tailoring the oceanic set-up for the coastal region and identify the remaining knowledge gaps.
We further understand that one of the main reviewer's concerns relates to the choice of validating the results using a database that largely overlaps with the one used to calibrate the model. Following his recommendation, we modified our approach and, using the latest versions of both SOCAT (i.e. version 4) and LDEO (i.e. v2015), we have now created two entirely independent datasets: one for the calibration (named SOCAT*) and one for validation (LDEO*). These two datasets were generated by randomly assigning each measurement common to both original databases to either SOCAT* or LDEO* (see comment 3 below for further details on the new approach). Another important suggestion was to further elaborate on the comparison between the simulated pCO_2 field and the validation dataset. We thus created new maps displaying the mean residuals errors between the pCO_2 values generated by the SOM_FFN, on the one hand, and those extracted from LDEO* and SOCAT*, on the other hand. This representation allows for a more detailed analysis of the performance of the model. As suggested by the reviewer, histograms of residual errors were also computed for each biogeochemical province and will be discussed in the updated manuscript. In addition, we have also introduced a new predictor (wind speed), which helped improve the performances of the SOM_FFN compared to those presented in the previous version of the manuscript.

While there are comparisons and validations of the SOM-FNN approach it mostly in terms of a RMSE. It is unclear what impact the RMSE would have on the phenomena investigated. Other means of comparison of how well the approach works should be performed. Rödenbeck et al (2015) present some nice diagnostics that could be applied.

At very least examples of the distribution of errors in pCO_2 should be shown in histograms.

[1] We agree with the reviewer that the assessment of the performance of the model only relied on averaged biases and RMSE calculated for each biogeochemical province. In the updated manuscript, we propose to include maps presenting the average residual errors between the pCO_2 field generated by the model and pCO_2 data extracted from the calibration (SOCAT*) and validation (LDEO*) datasets. They are obtained by subtracting the observed values from model output in each grid cell for every month where observations are available. This representation not only allows to assess which regions provide the best match with the observations but also to identify where the simulated pCO_2 overestimates (positive values, in red on the figure below) or underestimates (negative values, in blue on the figure below) the field data. Moreover, as suggested by the reviewer, we introduce a new figure, presenting the distribution of the residual errors between the results of the SOM_FFN and LDEO* for each biogeochemical province. This figure reveals nearly Gaussian distributions of the residuals for every biogeochemical province with the exception of province P8, for which the spread is not only the highest (indicating the largest discrepancy between model and observations), but also slightly skewed toward high values, thus revealing a tendency to overestimate the observed pCO_2.

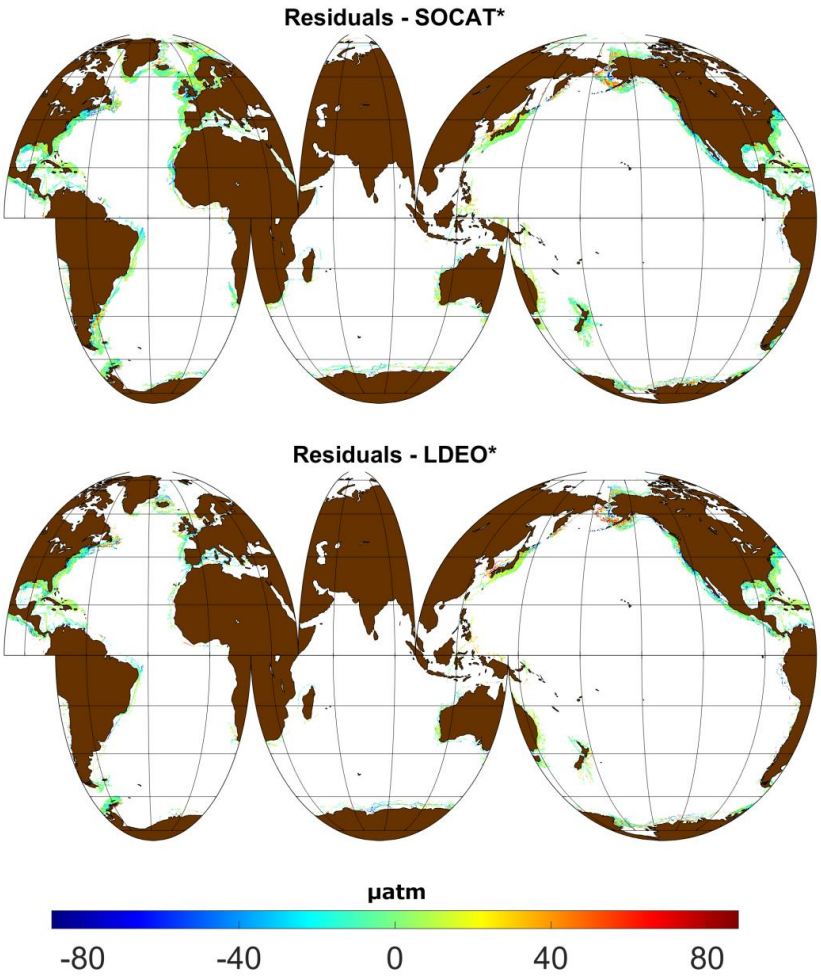

Figure 1: Mean residuals calculated as the difference between the SOM_FFM pCO_2 outputs and pCO_2 observations from SOCAT* (top) and LDEO* (bottom).

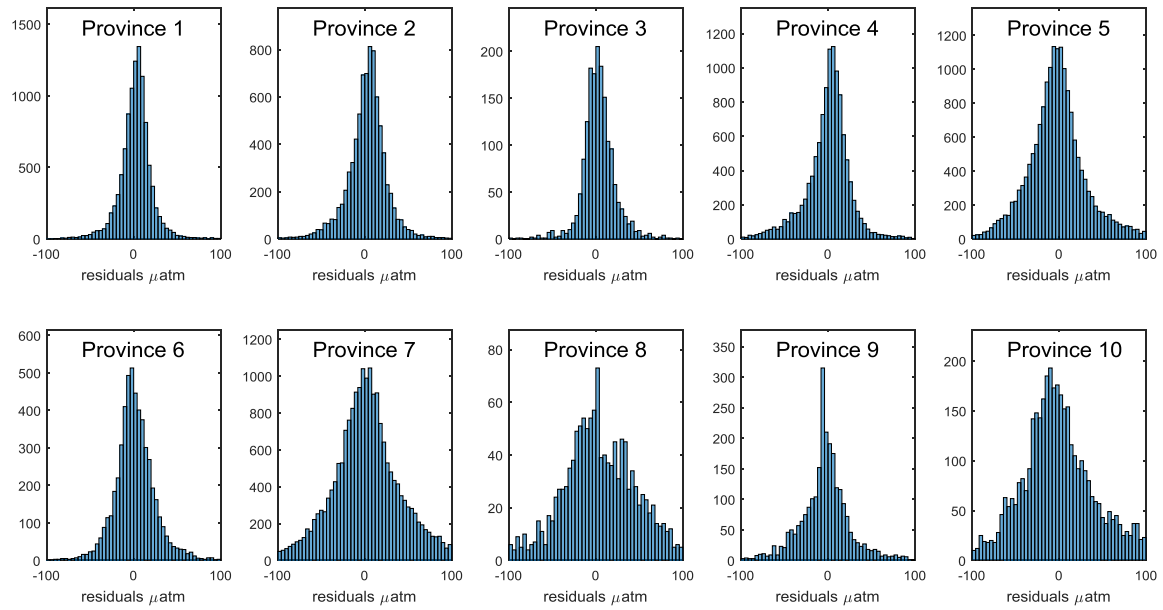

Figure: Histograms reporting the distribution of residuals between observed (LDEO*) and computed (SOM_FFN) pCO_2 in each biogeochemical province.

As the authors indicate, their definition of the coastal realm (200 nm or 1000 m depth) covers a much greater region than commonly viewed as coastal. The outer edge of the domain for much of the ocean can be considered "blue water". Therefor it is surprising that the differences between the coastal SOM-FFNN and open ocean SOM-FNN in Landschützer et al. are large. A more comprehensive diagnostic comparison should be made as it could suggest some fundamental issues with the approach.

[2] Although both the coastal SOM_FFN presented in this study and the oceanic SOM_FFN published in Landschützer et al. have a significant overlapping domains, they were not trained with the same datasets. For the most part, the coastal data from SOCAT used here to calibrate our model were not included in the data pool used for the open ocean simulations. In addition, the characteristic ranges of values within which both models are trained are also different for some of the environmental parameters. In particular, the average bathymetry and sea surface salinities are often significantly lower for data used. It is thus not surprising to observe significant differences between the results produced by both models, yet we agree with the reviewer that the magnitude of difference is somewhat interesting and highlights current knowledge gaps regarding the coastal ocean to open ocean transition zone. This certainly deserves some further investigation; however, we do believe that this is beyond the scope of this study. Nevertheless, in the updated manuscript, we will further discuss the differences between coastal and open SOM-FFN in the transition zone.

The validation approach is weak. There is significant (complete?) overlap between the data in SOCAT and that of Takahashi. The biases in datasets are likely due to different data reduction approaches. More comparisons should be made with actual data not used in the training, and more data should be excluded from the training for validation purposes.

[3] As mentioned by the reviewer, the SOCAT and LDEO databases have a large overlap, and the two datasets cannot be considered independent. In order to provide robust calibration and validation we now created two fully independent datasets based on SOCAT and LDEO, which do not contain any common measurement. We used the latest releases of both databases (i.e. SOCATv4 and LDEOv2015) and filtered out all non-coastal data points, as was already done in the previous version of the manuscript. Under our definition of the coastal zone, SOCATv4 contains ~8 10^6 data points and LDEO ~5.6 10^6, over 70% of which are also part of SOCATv4. We then randomly assigned each of those common data point to either database to insure that each data only belongs to one dataset. In the updated manuscript, the new datasets are renamed SOCAT* which is used to train the SOM_FFN, and LDEO* which is only used for validation purposes. In the new manuscript, the procedure used to create SOCAT* and LDEO* will be detailed in section 2.2 (Data Sources and processing).
The use of a more robust validation did not alter significantly the performances of the SOM_FFN and, combined with the inclusion of wind speed as a new predictor, the biases and RMSE generated by the model when compared with LDEO* are actually slightly lower than those presented in the original simulations (see table below). Also, note that the use of SOCATv4 and LDEOv2015 provides a significant number of data for the year 2015, which motivated us to expend our simulation period from 17 to 18 years.

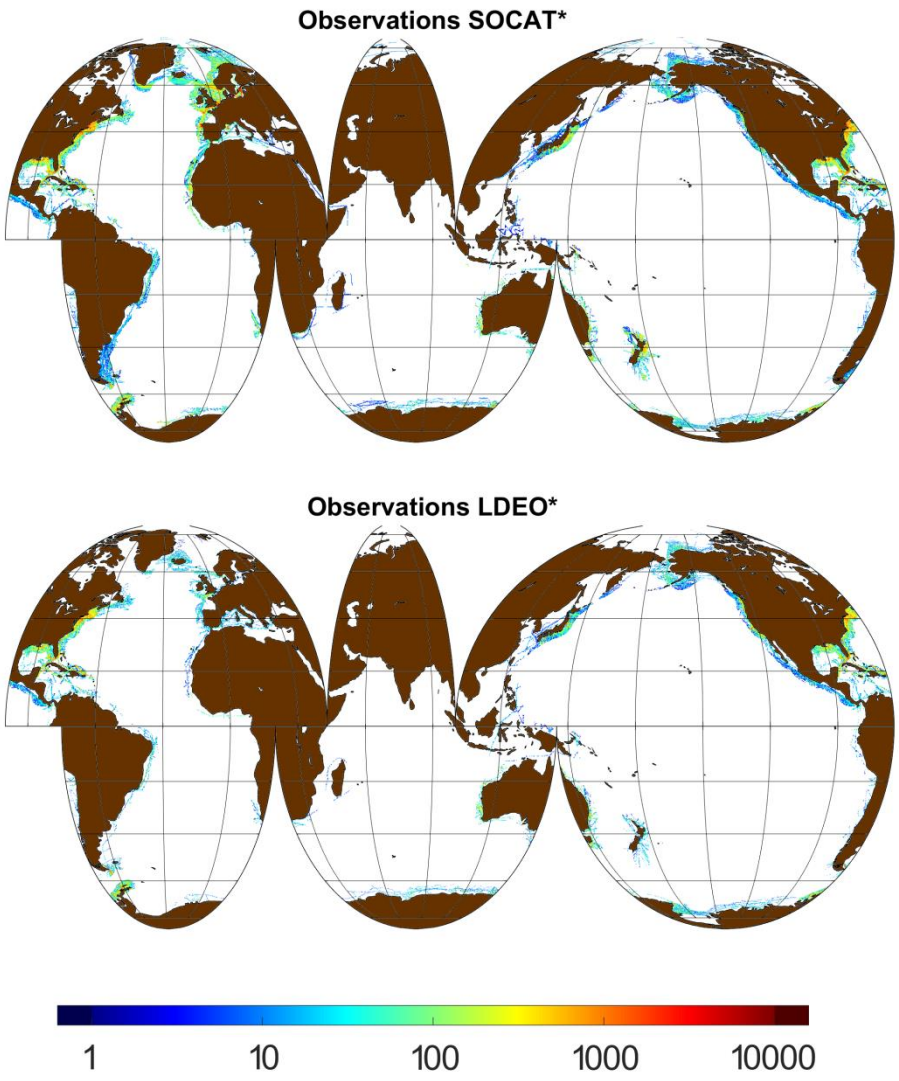

Figure: Number of observations contained in each 0.25° grid cell of the SOCAT* (top) and LDEO* (bottom) databases.

Table: Root mean squared error between observed and calculated pCO_2 in the different biogeochemical provinces. The SOM-FFN results are compared to data extracted from the SOCAT* and the LDEO* databases.

	SOCAT*		LDEO*	
Province	**Bias (µatm)**	**RMSE (µatm)**	**Bias (µatm)**	**RMSE (µatm)**
P1	0.0	19.1	2.0	20.5
P2	0.2	24.7	1.3	27.2
P3	-0.3	16.1	2.3	22.7
P4	-0.2	31.2	-1.6	33.0
P5	0.0	34.2	-1.4	38.0
P6	0.0	24.3	1.3	27.9
P7	0.1	37.2	-0.2	52.5
P8	0.2	46.8	3.9	51.4
P9	-0.1	23.0	-2.5	33.4
P10	0.0	35.7	1.6	53.1
Global	0.0	32.9	0.0	39.2

It is unclear how the change in surface water over time is dealt with. Are the pCO_2 data normalized like in the Takahashi monthly climatology? SST and SSS from the WOA are used but are these monthly climatologies that do not reflect change over time. This exercise provides monthly maps from 1998-2014 and it is clear how this is done. Also, the product is referred to as a climatology but it sounds like it is a monthly time series. That is, climatology mostly refers to a (multi) decadal average.

[4] During the training of the SOM_FFN, all pCO_2 data from SOCAT* are associated to a set of environmental conditions corresponding to the location and moment in time when the pCO_2 was measured. The relationships linking pCO_2 to environmental conditions as established by the FFN are then applied in each cell of the simulation domain for each of the 216 month of the simulation period. The inputs used for these calculations are 3 dimensional fields (latitude, longitude and time) containing values for each grid cell at every monthly time step. We will make sure to clarify this procedure in the updated manuscript. All the data used as inputs for both SOM and FFN are thus monthly times series and no normalization was applied to the data as was performed in Takahashi et al. (2009).
We realize that our frequent use of the word climatology may be misleading as to what our product really is. In the updated manuscript and the abstract, we will state more clearly that our calculations are performed for every month of the simulation period and thus produce monthly maps for each of the years simulated. Only then, a monthly climatology is derived from those results.
Also note that, in the new simulations, SST and SSS data are not taken from the World Ocean Atlas anymore but from the Met Office's EN4: quality controlled subsurface ocean temperature and salinity profiles and objective analyses (Good et al., 2009). This change was implemented following a comment from reviewer #2 regarding mismatches in spatial resolution of some datasets (the new SST/SSS datasets are at the spatial resolution of 0.25 degree as opposed to WOA which only provides values at 1 degree).

The grouping of provinces such that a coastal region can include an inshore and open ocean province is odd. Perhaps limit the coastal area to just one province

[5] The biogeochemical provinces generated by the Self Organizing Maps regroup ensembles of cells together because of similarities in their environmental characteristics. Within each biogeochemical province, however, some variability can be found and, while bathymetry may significantly contribute to the grouping of cells within a given province, so do the other environmental parameters (i.e. SSS, SST, wind speed and sea ice). As a consequence, some provinces have an extension that includes nearshore and more open waters but for which the range of temperature for example might be limited (see figure below displaying the spatial extent of the updated biogeochemical provinces). The choice to use the SOM and divide the coastal ocean into several provinces as was done for the open ocean in Landschützer et al. (2013) was motivated by the large variety of environmental settings that can be found in the coastal ocean. The current number of 10 provinces was selected as the optimal number during the calibration phase. When developing the model, several simulations were performed with the SOM using increasing numbers of biogeochemical provinces (from 6 to 20) and 10 was the number of biogeochemical provinces yielding the best results in terms of RMSE when compared with both SOCAT and LDEO databases. This number of biogeochemical provinces also guarantees that sufficient data will be located in each biogeochemical province, thus insuring both a proper training of the algorithm and the possibility of a validation against a significant number of observations. For instance, the spatio-temporal distribution of the biogeochemical provinces used in our last simulation allows for at least 1000 different grid cells to be used for validation against LDEO*.

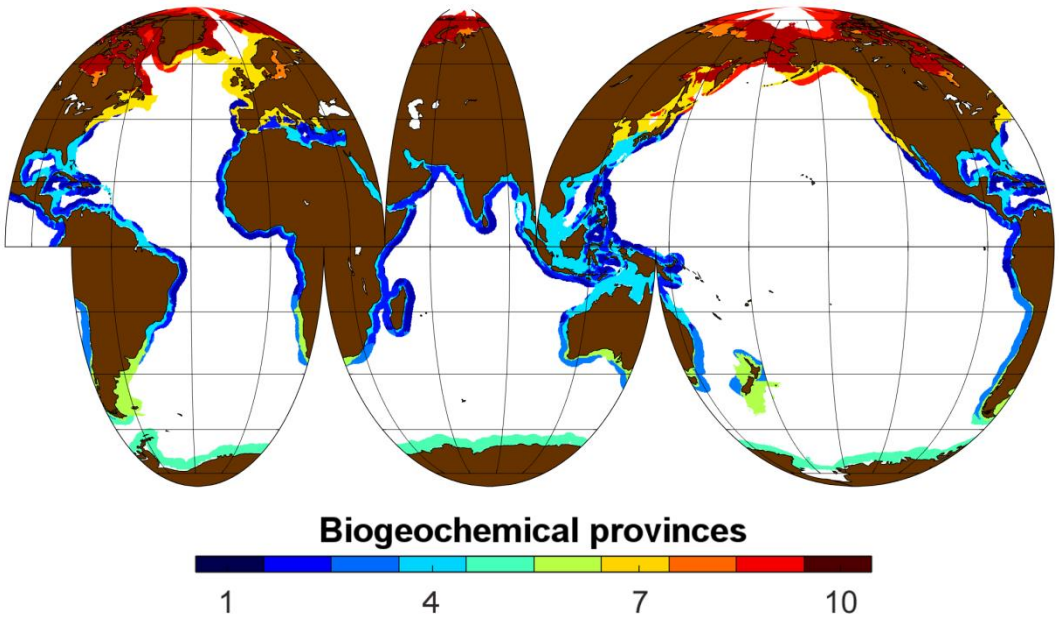

Figure 1: Map of the 10 different biogeochemical provinces generated by the SOM.

It is difficult to assess the data density for the different provinces using as validation or training.

[6] We understand the reviewer's concern and agree that, in the original version of the manuscript, limited information was provided regarding the spatial distribution of the

pCO_2 data used for calibration or validation. In the updated manuscript, a new figure (see comment [3]) now shows the data density of the SOCAT* and LDEO* databases for each grid cell of the simulation domain, thus providing a clear view of the amount and spatial distribution of data used both for calibration and validation..

Specific comments often relating to the general observations are below. The referenced text is in italics:
Line 125:" *motivated a number of modifications of the global ocean SOM-FFN method, including a 16 fold increase in spatial resolution from 1 degree to 0.25 degree, the introduction of a second neuron layer in the FFN calculations, the addition of new environmental variables as biogeochemical predictors, and a shortening of the simulation period to the period 1998 through 2014, rate of sea ice SST, SSS, bathymetry, sea-ice concentration and chlorophyll a second artificial neuron layer*". Some more detail on how these modification impact the results would be worthwhile .

[7] As mentioned by both reviewers, the different modifications introduced compared to the original set-up of the global ocean SOM_FFN are only mentioned in our method section but not discussed in details in our results. In the updated manuscript, we discuss the impact of those modifications (i.e. resolution and new predictors such as sea ice and wind speed). For instance, the added value of performing our simulations at the spatial resolution of 0.25° is discussed using examples such as the ability of our model to capture the plumes of larges rivers such as the Amazon, which produces an area located North of its river mouth characterized by pCO_2 values significantly lower than those of the surrounding waters (Cooley et al., 2007; Ibanez et al., 2015). The new discussion will also involve the addition of results from simulations performed only using SST, SSS, bathymetry and chlorophyll as predictors (as suggested by reviewer #2). The results of those simulations are presented in the table below and allow quantifying how the addition of new predictors affects the performance of the model. For instance, it can be noticed that, overall, the global RMSE increase significantly (from 39.2 to 48 µatm in the comparison with LDEO* when chlorophyll, sea ice and wind speed are not taken into account and from 39.2 to 45 µatm when only sea ice and wind speed are not taken into account). This deterioration of the performance of the model, however, is not evenly affecting all provinces and it can be observed in particular that provinces located at high latitudes (i.e. P8, P9 and P10) perform significantly worse without the inclusion of wind speed and sea ice.

Table: Biases and root mean squared error (RMSE) between observed and calculated pCO_2 using only SST, SSS and bathymetry (STB) or SST, SSS, bathymetry and chlorophyll (STBC) as predictors.

	SOCAT*				**LDEO***			
Province	**Bias (µatm)**		**RMSE (µatm)**		**Bias (µatm)**		**RMSE (µatm)**	
	STB	STBC	STB	STBC	STB	STBC	STB	STBC
P1	0.0	-0.2	20.8	21.0	2.4	2.0	21.7	21.5
P2	-0.1	0.1	26.9	27.8	0.5	0.8	29.0	29.6
P3	0.0	-0.5	22.7	21.3	3.0	2.3	27.1	26.8
P4	0.0	-0.2	33.0	33.0	-1.7	-2.3	33.8	33.8
P5	0.2	0.1	52.7	42.2	-1.7	-0.9	56.9	44.5
P6	0.0	0.1	26.8	26.5	-0.5	0.6	28.9	28.0
P7	0.4	0.3	44.3	44.1	1.2	0.3	59.3	58.8

P8	0.1	0.4	82.6	80.0	9.1	9.0	56.3	58.5
P9	0.1	0.9	34.7	36.5	-2.6	-2.8	39.8	41.8
P10	-0.3	0.7	49.8	49.5	-3.9	-3.0	76.5	75.4
Global	0.1	0.2	43.9	42.4	0.0	0.0	48.0	45.0

Line 175: "*SOM-FFN from generating negative values*." This suggests that there are issues with the original setup. Adding a second neuron layer to prevent negative values certainly is unorthodox.

[8] The SOM-FFN method is some form of a non-linear regression model, which in cases of bad conditioning also produces out of range values. We point here that the negative values do not suggest issues with the model as a whole, but rather issues with the setup of the model. While we did not face the problem of negative values using a standard hidden layer in the open ocean, the added complexity combined with little data in certain province can cause this behaviour in coastal seas. For instance, there exist very few measurements for shallows waters with very low salinity and high sea ice coverage. Faced with conditions for which it was not trained, the SOM_FFN does not perform ideally and may generate unrealistic values. In our original manuscript we solved this by introducing a second hidden layer of neurons, however, we found a more stable solution in terms of negative values, i.e we replaced the second neuron layer with the use of a sigmoid activation function bounded between 0 and 1 (normalized pCO_2 units) in the hidden layer. This means that per definition our results are bound to stay above 0. The implementation of this solution did not deteriorate the overall results but prevented the SOM_FFN from generating negative pCO_2 values. The new simulations for the revised manuscript were thus carried out with this new setting, which now only uses a single neuron layer.

Line 193: "*All the datasets used in our calculations were converted from their original spatial resolutions to a regular 0.25 degree resolution grid*." Specify what the original resolution was for each dataset.

[9] A more thorough description of the datasets used in the study will be included into section 2.2 (Data Sources and processing). This description explicitly states the original temporal and spatial resolution of each dataset used. This information will be compiled in the new table reported below. In addition, for the sake of reproducibility, a link toward all datasets used will be provided in the 'Data Availability' section at the end of the manuscript. Note that, as already reported in comment 4, all our products have now an original resolution of 0.25° or finer.

Table: Datasets used to create the environmental forcing files. The original spatial and temporal resolution and the main manipulations applied for their use in the SOM_FFN are also reported.

Predictor	dataset	resolution	reference	Manipulation
SST	EN4	0.25°, daily	Good et al., 2013	Monthly average
SSS	EN4	0.25°, daily	Good et al., 2013	Monthly average
Bathymetry	ETOPO2	2 minutes	US Department of Commerce,	Aggregation to 0.25°

Sea ice	NSIDC	0.25°, monthly	2006 Cavalieri et al., 1996	Monthly rate of change in sea ice coverage
Chlorophyll a	SeaWifs, MODIS	9km, monthly	NASA, 2016	Aggregation to 0.25°
Wind speed	ERA	0.25°, 6hours	Dee et al., 2011	Monthly average

Line 196: "*SST and SSS maps were taken from the World Ocean Atlas (Antonov et al., 2010 for SST and Locarnini et al., 2010 for SSS)*." Are these monthly climatologies or monthly time series? If the former it is unclear how the time element from 1998-2014 is incorporated.

[10] The new simulations do not use SST and SSS from the World Ocean Atlas anymore but from the Met Office's EN4: quality controlled subsurface ocean temperature and salinity profiles and objective analyses (Good et al., 2009). Those data are time series and contain individual values in each grid cell of the simulation domain for each of the 216 month of the simulation period. Additional information regarding the incorporation of the time element in our calculation is included in answer [4] and the updated manuscript will be more explicit with respect to the way our calculations are performed.

Line 203 and beyond: " *validation are extracted from the LDEOv2014 database The coastal SOM-FFN results are validated through a comparison with the LDEOv2014 data (Takahashi et al., 2016)*." This is not independent data and not a proper validation in statistical sense.

[11] As discussed in the answer to reviewer's comment [3], we fully agree that the original validation was significantly weakened by the large overlap between SOCAT and LDEO. Now that we created two entirely independent datasets to train the model (SOCAT*) and evaluate its performances (LDEO*), we believe that the term "validation" is now appropriate for the updated manuscript.

Line 280: "*Considering these complexities, the achieved RMSE is quite good*." Two issues here. How are the complexities determined? That is, we know the coastal region is complex but it is unclear if the complexity is incorporated into the analysis using T, S, chl-a and sea ice. And, based on what criteria is the RMSE quite good.

[12] It is true that the coastal region is known to be a complex environment and that was the main message of this sentence. Whether our analysis capture the intricate complexity of the coastal zone has to be indeed better discussed in the revised manuscript. We will thus further develop the section dedicated to the discussion and quantification of the effects induced by modifications in SOM_FFN configuration on its performance (see answer to comment [7]). With respect to the RMSE, our criteria to consider the performance of our model 'quite good' is the comparison with the RMSE reported in regional studies . This is further discussed in the answer [13] below.

Line 306:" *which compares with the most robust pCO2 regional coastal estimates from the literature (Chen et al., 2016*)". Chen et al. 2016 use a crude remote sensing approach. These are by no means "most robust".

[13] The paper by Chen et al. (2016) indeed presents pCO_2 fields for the Western Florida shelf generated using remote sensing. Such methodology certainly is different and arguably less sophisticated that the method described in our study. However, we did not mean to directly compare the performance of our model with those of Chen et al. (2016). Our aim was to find as many recent studies as possible to compare our results and to gain some confidence in our estimates. Their study reports (table 1, page 12) a list of regional coastal models generating pCO_2 fields derived from other environmental factors. Although the methods used in this list varies greatly (including Mutiple Linear Regressions, Mechanistic semi analytical models and Self Organizing Maps), we believe it was relevant to confront the performance of our model applied globally with those of other coastal models, which are only applied at regional scale in well covered areas. What we meant to say is that there exist a body of literature using various methodological approaches to generate pCO_2 fields and the article by Chen was mostly used for his table. Nevertheless, following the reviewer's comment, we will tone down our statement that our results compare with the most robust estimates from the literature. Rather, we'll state that the RMSE calculated in our best constrained biogeochemical provinces (i.e. in the 20-30 µatm range for P1, P2, P3 and P6) can be compared with those obtained by regional models applied in well monitored areas.

Line 349: "*highlight the current knowledge gap regarding the mean state and variability of the transition zone.* " It is unclear if this highlights a knowledge gap or highlights issues wit the SOM_FNN approach. This warrants some discussion

[14] We agree with the reviewer's comment (as well as similar concerns' raised by reviewer 2) and recognise that the original version of the manuscript only briefly compared the results of the updated coastal SOM_FFN with those of the original oceanic model. In the updated manuscript, a more in depth comparison with the results of the open ocean configuration will be provided. This will allow better identifying the added value of the modifications done to the SOM_FFN method in our study and help clearly identify remaining knowledge gaps.

Line 358: "*Our results indicate that the very nearshore processes controlling the CO2 dynamics likely*" Again the SOM-FNN is a mathematical construct. So I guess what the authors are stating is that the SOM-FNN cannot address adequately nearshore dynamics.

[15] The reviewer is correct; this sentence was meant to stress that, in spite of the improvement provided by the new method, some very nearshore processes still cannot be addressed perfectly. As the reviewer pointed out, the problem does not lie with the mathematical approach used by the spatial resolution required to capture very nearshore processes. The sentence was rephrased as follows:
"***Overall, the occurrence of large residuals in the shallowest cells of our calculation domain in*** our results ***(fig. 2) suggest*** that the very nearshore processes controlling the CO_2 dynamics likely are the most difficult to reproduce ***at the global scale.***"

Line 429 "2 ". The "n" generally refers to salinity normalization. Perhaps use pCO2(SSTmean) .

[16] We will follow the reviewer's suggestion in the updated manuscript and use pCO_2(SSTmean) instead of $npCO_2$.

Line 470: "*cells at a 0.25° spatial resolution for each of the 204 month of the simulation period (from January 1998 to December 2014). Climatologically averaged pCO2 maps for each month are*". The use of the term climatology is ambiguous here.

[17] We agree with the reviewer, the term climatology is ambiguous in this sentence and elsewhere. To avoid any confusion, the paragraph was rephrased as follows:

"The data product associated to this manuscript consists of a netcdf file containing the pCO_2 for ice-free cells at a 0.25° spatial resolution for each of the ***216*** month of the simulation period (from January 1998 to December ***2015***). ***12 maps representing mean pCO_2 fields calculated for each month over the simulation period*** are also provided."

Line 471: The province names are peculiar "Deep Polar, Polar Very deep Polar"

[18] Our choice of names for the different biogeochemical provinces was only meant to outline their main geographical distribution. Both reviewers commented on the lack of added value of the distributions of the biogeochemical provinces. In the updated manuscript, the biogeochemical provinces will only be referred to as P1, P2 and so on to avoid confusion. Section 3.1 however, will still discuss the spatial extent of the each biogeochemical province.

Table 1 suggests that Ice is a predictor in the tropics?

[19] We agree that the use of Ice as predictor in the tropics is not relevant, however Ice cover in the tropics in our predictor dataset was 0 at all times, and hence it did not influence the neural network. To avoid confusion, in the updated simulation, Ice is only a predictor in provinces P5 to P10, in which at least partial seasonal ice coverage is reported.

Table 2: List of the biogeochemical provinces, their geographic distribution and the environmental predictors used to calculate surface ocean pCO_2. SSS stands for sea surface salinity, SST for sea surface temperature, Bathy for bathymetry, Ice for sea-ice cover, Chl for chlorophyll concentration ***and Wind for wind speed***.

Province	SSS	SST	Bathy	Ice	Chl	Wind
P1	**X**	**X**	**X**		**X**	**X**
P2	**X**	**X**	**X**		**X**	**X**
P3	**X**	**X**	**X**		**X**	**X**
P4	**X**	**X**	**X**		**X**	**X**
P5	**X**	**X**	**X**	**X**	**X**	**X**
P6	**X**	**X**	**X**	**X**	**X**	**X**
P7	**X**	**X**	**X**	**X**	**X**	**X**

P8	**X**	**X**	**X**	**X**	**X**
P9	**X**	**X**	**X**	**X**	**X**
P10	**X**	**X**	**X**	**X**	**X**

Also P3 and P4 appear to have the same "distribution".

[20] In the original simulations, provinces P3 and P4 did not display exactly the same spatio-temporal distribution but were both referred to as “Deep Tropical” which could indeed lead to confusion. Actually, the average water depth of cells included in P4 was deeper than that of those included in P3 and, P4 generally characterized more ‘open waters’. As mentioned in answer [5], the updated manuscript will describe and discuss the spatial distributions of the 10 biogeochemical provinces but the restrictive ‘distributions’ will be removed from table 1.

Figure 1 shows a peculiar extension off of New Zealand. Is this the Chatham Rise and is this considered coastal?

[21] The extension Southward and Eastward of New Zealand are the Campbell Plateau and Chatham Rise, respectively. They are considered coastal following our ‘extended’ definition of the continental shelf and upper slope because they are characterized by depth shallower than 1000m (our outer limit) and connected to a continental platform.

Figure 2: Perhaps comment on the absence of high pCO_2 in the SOM-FNN for the summer monsoon upwelling region in the Arabian Sea. Data of the Takahashi climatology clearly show this. Figure 2 does not show the high pCO_2 Arabian Sea seasonal (JAS) upwelling off the coast of the Arabian Peninsula.

[22] It is true that high pCO_2 values have been regularly observed along the coast of the Arabian Sea (Sarma et al., 2003) and are considered to be the consequence of monsoon driver upwelling occurring in the region. As noted by the reviewer, the SOM-FFN does not reproduce these oversaturated waters. We now mention and discuss the inability of the SOM_FFN to reproduce this known feature of the Arabian shelf in section 3.3.1, which discusses the general spatial patterns of the pCO_2 fields generated by the model.

Literature cited in the responses:

Cavalieri, D. J., Parkinson, C. L., Gloersen, P., and Zwally, H.: Sea Ice Concentrations from Nimbus-7 SMMR and DMSP SSM/I-SSMIS Passive Microwave Data, years 1990–2011, NASA DAAC at the Natl. Snow and Ice Data Cent., Boulder, Colo. (Updated yearly.), 1996.

Chen, S., Hu, C., Byrne, R. H., Robbins, L. L., and Yang, B.: Remote estimation of surface pCO2 on the West Florida Shelf, Continental Shelf Research, 128, 10–25, 2016.

Cooley, S. R., V. J. Coles, A. Subramaniam, and P. L. Yager (2007), Seasonal variations in the Amazon plume-related atmospheric carbon sink, Global Biogeochem. Cycles, 21, GB3014, doi:10.1029/2006GB002831.

Dee, D. P., Uppala, S. M., Simmons, A. J., Berrisford, P., Poli, P., Kobayashi, S., Andrae, U., Balmaseda, M. A., Balsamo, G., Bauer, P., Bechtold, P., Beljaars, A. C. M., van de Berg, L., Bidlot, J., Bormann, N., Delsol, C., Dragani, R., Fuentes, M., Geer, A. J., Haimberger, L., Healy, S. B., Hersbach, H., Hòlm, E. V., Isaksen, L., Kallberg, P., Köhler, M., Matricardi, M., Mcnally, A. P., Monge-Sanz, B. M., Morcrette, J. J., Park, B. K., Peubey, C., de Rosnay, P., Tavolato, C., Thépaut, J. N. and Vitart, F.: The ERA-Interim reanalysis: Configuration and performance of the data assimilation system, Q. J. R. Meteorol. Soc., 137(656), 553–597, doi:10.1002/qj.828, 2011.

Good, S. A., M. J. Martin and N. A. Rayner, 2013. EN4: quality controlled ocean temperature and salinity profiles and monthly objective analyses with uncertainty estimates, Journal of Geophysical Research: Oceans, 118, 6704-6716, doi:10.1002/2013JC009067

Ibánhez, J. S. P., D. Diverrès, M. Araujo, and N. Lefèvre (2015), Seasonal and interannual variability of sea-air CO2 fluxes in the tropical Atlantic affected by the Amazon River plume, Global Biogeochem. Cycles, 29, 1640–1655, doi:10.1002/2015GB005110.

Landschützer, P., Gruber, N., Bakker, D. C. E., Schuster, U., Nakaoka, S., Payne, M. R., Sasse, T., and Zeng, J.: A neural network-based estimate of the seasonal to inter-annual variability of the Atlantic Ocean carbon sink, Biogeosciences, 10, 7793-7815, doi:10.5194/bg-10-7793-2013, 2013.

NASA Goddard Space Flight Center, Ocean Ecology Laboratory, Ocean Biology Processing Group; (Dataset Release 2016): MODIS-Aqua chlorophyll Data; NASA Goddard Space Flight Center, Ocean Ecology Laboratory, Ocean Biology Processing Group, 2016.

Sarma, V. V. S. S., Monthly variability in surface pCO2 and net air-sea CO2 flux in the Arabian Sea, J. Geophys. Res., 108 (C8), 3255, doi:10.1029/2001JC001062, 2003.

Takahashi, T., S. C. Sutherland, R. Wanninkhof, C. Sweeney, R. A. Feely, D. W. Chipman, B. Hales, G. Friederich, F. Chavez, A. Watson, D. C. E. Bakker, U. Schuster, N. Metzl, H. Yoshikawa-Inoue, M. Ishii, T. Midorikawa, Y. Nojiri, C. Sabine, J. Olafsson, Th. S. Arnarson, B. Tilbrook, T. Johannessen, A. Olsen, Richard Bellerby, A. Körtzinger, T. Steinhoff, M. Hoppema, H. J. W. de Baar, C. S. Wong, Bruno Delille and N. R. Bates (2009). Climatological mean and decadal changes in surface ocean pCO2, and net sea-air CO2 flux over the global oceans. Deep-Sea Res. II, 56, 554-577

U.S. Department of Commerce, National Oceanic and Atmospheric Administration, National Geophysical Data Center. 2006. 2-minute Gridded Global Relief Data (ETOPO2v2). http://www.ngdc.noaa.gov/mgg/fliers/06mgg01.html. Accessed 21 May 2017.

Review of bg-2017-64 “Global high-resolution monthly pCO2 climatology for the coastal ocean derived from neural network interpolation” by Laruelle et al.

This manuscript proposed a modified two-step artificial neural network method for deriving pCO2 (SOM-FFN, Landschützer et al., 2013), and focused on shelf seas. The most important modification are (1) much higher resolution as 0.25 degree; (2) inclusion of sea-ice as a predictor of pCO2. From this effort, the authors may present a fine scale coastal sea pCO2 globally, as Fig. 2 in the manuscript shown. This is certainly of value. However, there are some major issues. The method is not new, rather an interpolation of the open ocean model.

We are pleased to see that the reviewer values our coastal pCO_2 maps and are grateful for his constructive remarks and suggestions. We understand that the reviewer is not fully convinced by the novelty of the method and the added value our manuscript under its current form. As explained in answers, we do not concur with the statement that our model only is an extension or interpolation of the previously existing oceanic model. Instead, we believe that it is a significantly modified version, specifically tailored to reconstruct the complex coastal pCO_2 cycle. In the updated manuscript, we propose to put more emphasis on the modifications of the original SOM_FFN and compare our coastal set up with the open ocean one. Further attention will also be given to better quantifying the improvements resulting from the modification of the open ocean set-up from Landschützer et al. (2013) and identifying the remaining knowledge gaps (see also replies to comments 2, 7, 14 of reviewer 1).
The reviewer was also concerned by the weakness of the validation of our results performed using a database that largely overlaps with the database used to calibrate the model. Following both reviewer’s recommendations, we modified our approach and, using the latest versions of both SOCAT (i.e. version 4) and LDEO (i.e. v2015), we created two entirely independent datasets, named SOCAT* for the calibration and LDEO* for the validation. These two datasets were generated by randomly assigning each measurement common to both original databases to either SOCAT* or LDEO* (see comment 2 below for further details on the new approach). In addition, we have also introduced a new predictor (wind speed), which helped improve the performances of the SOM_FFN compared to those presented in the previous version of the manuscript.
Please find bellow a detailed answer to each comment. All our answers are written in blue and the modifications within the text are highlighted in bold and italic.
On behalf of all co-authors,

Goulven Laruelle

It was said that all data were converted to 0.25 degree from their original resolution. Then please indicate clearly original resolution of each data, for example, SSS, SST and depth. At least for SST and SSS from the World Ocean Atlas, I wonder if the resolution is fine in the shelf seas (sorry I do not
check, my memory is 1 degree). If it is true, I do not think such an interpolation of SST and SSS would help in deriving really high resolution pCO2 (i.e. the final result might be close to a simple interpolation of modeling pCO2 of 1 degree resolution).

[1] The spatial resolution of SST and SSS from the World Ocean Atlas is indeed only 1 degree. In response to the reviewer’s comment, we now apply 0.25° resolution datasets

for SSS and SST by using Met Office's EN4: quality controlled subsurface ocean temperature and salinity profiles and objective analyses (Good et al., 2009). By doing so, all predictors used for the calculation of the SOM_FFN have now resolution of 0.25° or higher. We also propose the inclusion of the table below, which lists the selected datasets used, their purpose (i.e. calibration, validation…) and original spatio-temporal resolution.

We reiterate here that we disagree with the notion that our model is a mere interpolation of the global oceanic model developed by Landschützer et al. (2013). Although both the coastal SOM_FFN presented in this study and the oceanic SOM_FFN published in Landschützer et al. (2013) share common methodologies, they were not trained with the same datasets. For the most part, the coastal data from SOCAT used here for calibration and validation was not included in the data pool used for the open ocean simulations. In addition, the ranges of values (within which both models are trained) are also different for some of the environmental parameters. In particular, the average bathymetry and sea surface salinities are often significantly lower in coastal regions than in the open ocean. We thus believe that the important physical and biogeochemical differences between coastal and open oceanic waters fully justify careful retraining of the SOM_FFN. In addition, the typical spatial scales of physical and biogeochemical gradients in nearshore waters are often smaller than 1 degree and justify the implementation of the SOM_FFN at a higher resolution. Nevertheless, to better demonstrate the value of our approach, we follow the comment of the reviewer and discuss in more details the comparison between open and coastal ocean models in the revised manuscript.

Table 1: Datasets used to create the environmental forcing files. The original spatial and temporal resolution and the main manipulations applied for their use in the SOM_FFN are also reported.

Predictor	dataset	resolution	reference	Manipulation
SST	EN4	0.25°, daily	Good et al., 2013	Monthly average
SSS	EN4	0.25°, daily	Good et al., 2013	Monthly average
Bathymetry	ETOPO2	2 minutes	US Department of Commerce, 2006	Aggregation to 0.25°
Sea ice	NSIDC	0.25°, daily	Cavalieri et al., 1996	Monthly rate of change in sea ice coverage
Chlorophyll a	SeaWifs, MODIS	9km, monthly	NASA, 2016	Aggregation to 0.25°
Wind speed	ERA	0.25°, 6hours	Dee et al., 2011	Monthly average

SOCAT was used for tuning the model and LDEO was used for validation, while the two dataset was largely overlapped. This is not allowed for developing a sound and solid approach.Randomly picking data from SOCAT for calibration, and then removing those data at the same location when picking the LDEO data for validation, would not be too hard to do.

[2] As mentioned by the reviewer, the SOCAT and LDEO databases have a large overlap, and the two datasets cannot be considered independent. In order to remedy to this problem, we followed the reviewer suggestion and created two datasets based on SOCAT and LDEO which do not contain any common measurements. We used the latest releases of both databases (i.e. SOCATv4 and LDEOv2015) and filtered out all non-coastal data points, as it was already done in the previous version of the manuscript. Under our definition of the coastal zone, SOCATv4 contains ~8 10^6 data points and LDEO ~5.6 10^6, over 70% of which are also part of SOCATv4. We then randomly assigned each of those common data points to either database, thus insuring that each data only belongs to one dataset. In the updated manuscript, the new datasets are then called SOCAT* which is used to train the SOM_FFN, and LDEO* which is only used for validation purposes. In the new manuscript, the procedure used to create SOCAT* and LDEO* will be detailed in section 2.2 (Data Sources and processing).
The use of a more robust validation did not alter significantly the performances of the SOM_FFN and, combined with the inclusion of wind speed as a new predictor, the biases and RMSE generated by the model when compared with LDEO* are actually slightly lower than those presented in the original simulations (see table below). Also, note that the use of SOCATv4 and LDEOv2015 provides a significant number of data for the year 2015, which motivated us to expend our simulation period from 17 year to 18.

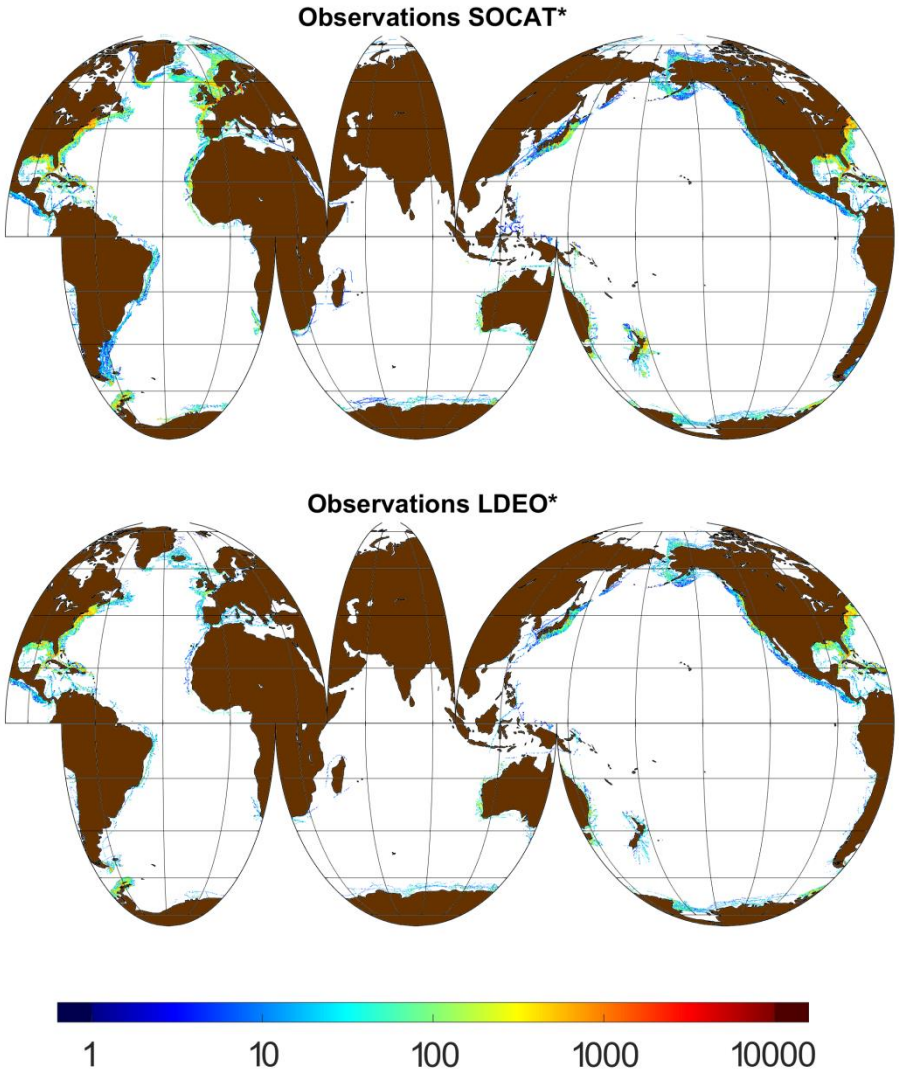

Figure: Number of observations contained in each 0.25° grid cell of the SOCAT* (top) and LDEO* (bottom) databases.

"Table: Root mean squared error between observed and calculated pCO_2 in the different biogeochemical provinces. The SOM-FFN results are compared to data extracted from the SOCAT* and the LDEO* databases.

	SOCAT*		LDEO*	
Province	**Bias (µatm)**	**RMSE (µatm)**	**Bias (µatm)**	**RMSE (µatm)**
P1	0.0	19.1	2.0	20.5
P2	0.2	24.7	1.3	27.2
P3	-0.3	16.1	2.3	22.7
P4	-0.2	31.2	-1.6	33.0
P5	0.0	34.2	-1.4	38.0
P6	0.0	24.3	1.3	27.9
P7	0.1	37.2	-0.2	52.5
P8	0.2	46.8	3.9	51.4
P9	-0.1	23.0	-2.5	33.4
P10	0.0	35.7	1.6	53.1
Global	0.0	32.9	0.0	39.2

The target of this manuscript is not clear. Based on the title, it looks that it is talking about a new product. As to the text, methods and validation are vague, while the authors are still eager to describe the seasonality and spatial distribution, but with no way to go into depth. And maybe because of no full confidence in the results, they frequently warned "considered with caution". I would suggest the authors focusing on method and validation, teasing each detail carefully, which would raise the merit of this study. Because one of the most important changes is to include ice, the authors need to show that by including ice, what was improved? What more was acquired/learned?

[3] The manuscript presents monthly pCO_2 fields for the coastal ocean generated by a statistical method that was never applied in such environment. Obviously, a large part of the manuscript is dedicated to presenting the methods (i.e. the modifications of the open ocean set up in order to better capture the dynamics of continental shelves) and we agree with the reviewer that each critical point of the method should be discussed thoroughly. Following his recommendation, we now discuss results obtained with our model ignoring our new predictors (wind speed and sea ice cover) to better quantify their contribution to the accuracy of our results. Similarly, the added value of performing our simulations at the spatial resolution of 0.25° is also discussed using examples such as the ability of our model to capture the plumes of larges rivers such as the Amazon, which produces an area located North of its river mouth characterized by pCO_2 values significantly lower than those of the surrounding waters (Cooley et al., 2007; Ibanez et al., 2015). We believe that this discussion will clearly allow the reader to understand the added value of our approach. In addition, the validation of our results is now much more developed by including maps of mean residuals obtained when comparing the pCO_2 field generated by the SOM_FFN with data from LDEO* and histograms of the distribution of these residuals with each biogeochemical province (see figures below).

However, we also believe that it is useful to thoroughly describe our results in terms of spatial and seasonal trends and not restrict our analysis to comparison against

validation data. One of the main values of our data product is the resolution of the seasonal variations of pCO_2 in regions of the continental shelf that were largely under sampled until now. We thus believe that, although the main purpose of our manuscript is to describe a new coastal pCO_2 data product, dedicating a significant fraction of our results and discussion to the emerging spatial and temporal patterns in the coastal pCO_2 field is justified and relevant. As for our warning that results in certain regions should be "considered with caution": Despite the increasing number of observations collected and the methodological advancements, there are still regions, such as the Siberian shelves, where only few observations exist and our process understanding is limited. Limited observations mean on the one hand limited information to train our model but on the other hand also only limited means to validate our results. This should not be misinterpreted as us having a lack of confidence, but rather us having limited means of validating our results for some areas of the global coastal ocean. With this statement, we wanted to highlight these limitations and help the reader to critically reflect on our results.

Table: Biases and root mean squared error (RMSE) between observed and calculated pCO_2 using only SST, SSS and bathymetry (STB) or SST, SSS, bathymetry and chlorophyll (STBC) as predictors.

	SOCAT*				**LDEO***			
Province	**Bias (µatm)**		**RMSE (µatm)**		**Bias (µatm)**		**RMSE (µatm)**	
	STB	STBC	STB	STBC	STB	STBC	STB	STBC
P1	0.0	-0.2	20.8	21.0	2.4	2.0	21.7	21.5
P2	-0.1	0.1	26.9	27.8	0.5	0.8	29.0	29.6
P3	0.0	-0.5	22.7	21.3	3.0	2.3	27.1	26.8
P4	0.0	-0.2	33.0	33.0	-1.7	-2.3	33.8	33.8
P5	0.2	0.1	52.7	42.2	-1.7	-0.9	56.9	44.5
P6	0.0	0.1	26.8	26.5	-0.5	0.6	28.9	28.0
P7	0.4	0.3	44.3	44.1	1.2	0.3	59.3	58.8
P8	0.1	0.4	82.6	80.0	9.1	9.0	56.3	58.5
P9	0.1	0.9	34.7	36.5	-2.6	-2.8	39.8	41.8
P10	-0.3	0.7	49.8	49.5	-3.9	-3.0	76.5	75.4
Global	0.1	0.2	43.9	42.4	0.0	0.0	48.0	45.0

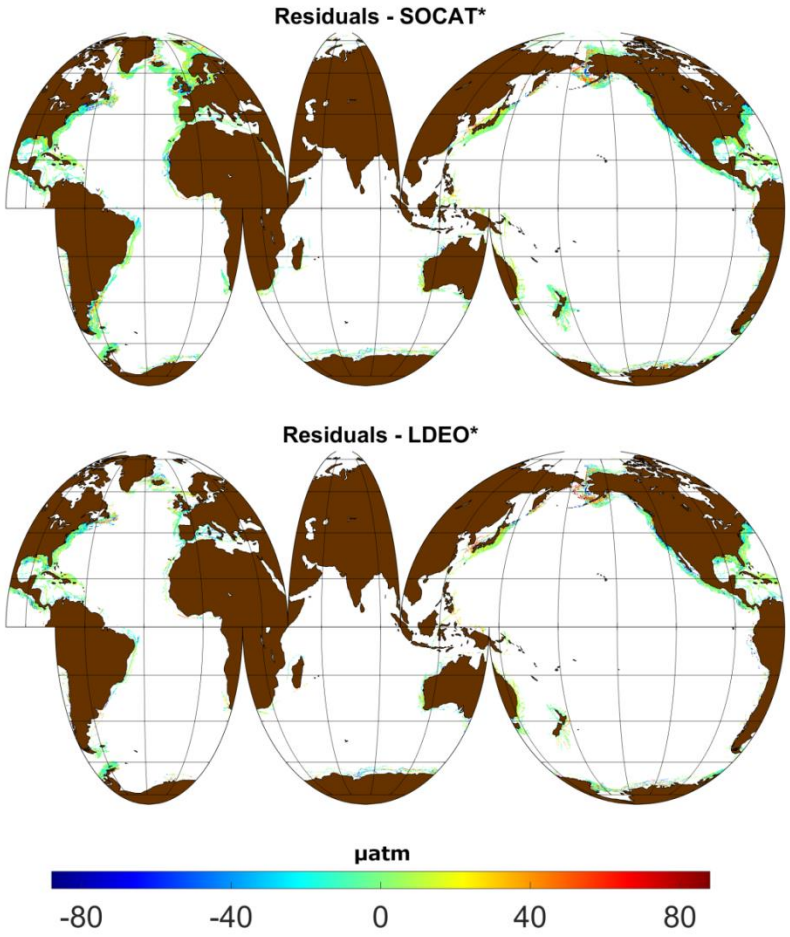

Figure 1: Mean residuals calculated as the difference between the SOM_FFM pCO_2 outputs and pCO_2 observations from SOCAT* (top) and LDEO* (bottom).

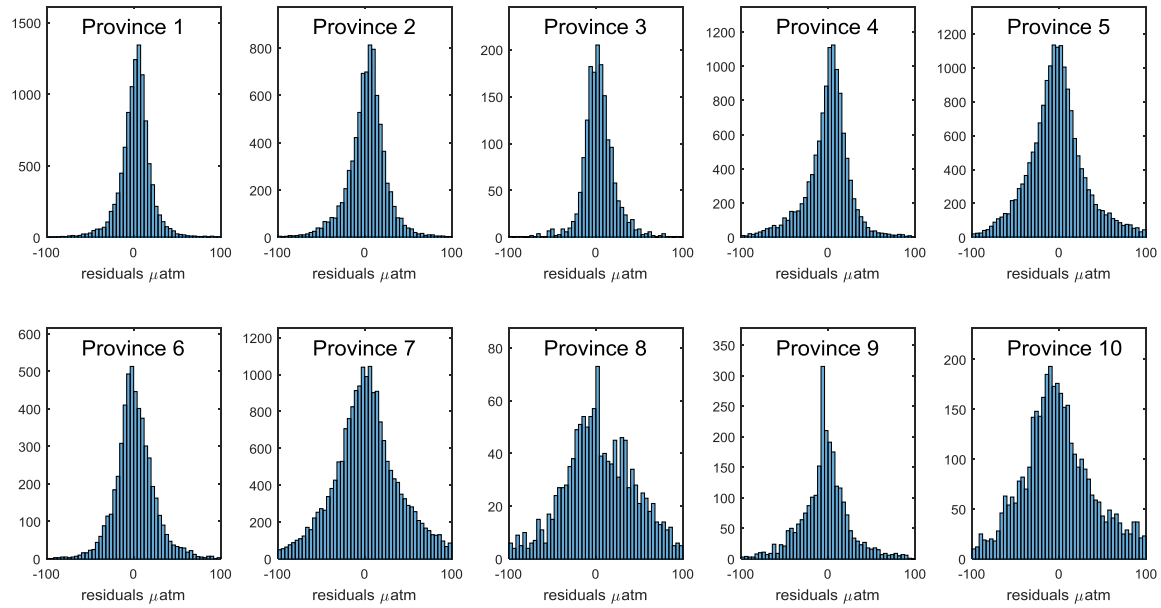

Figure: Histograms reporting the distribution of residuals between observed (LDEO*) and computed (SOM_FFN) pCO_2 in each biogeochemical province.

Specific comments: Abstract- Writing of the abstract needs to be improved. A very clear point should be delivered. People want to know by modifying an established algorithm, what has been acquired/improved and how good it is. Now the authors just say it is assessed using two datasets. Meridional distribution is confirmed. And then talking about seasonality produced from this dataset, which people do not know if it is true or not. If spatial and temporal variability are what the authors concerned, the title should be changed correspondingly.

[4] As mentioned in answer [3], the updated manuscript now dedicates more effort to better identifying what was improved and learned with each of the modification introduced to the SOM_FFN compared to its open ocean set up. Also, we now implemented a more robust validation of our results (following several suggestions of both reviewers), including a revised comparison with monthly climatological cycles extracted from LDEO* at 40 locations (see figure below). We thus do not agree with the reviewer when he suggests that our discussion regarding the seasonality of pCO_2 in coastal waters is unsubstantiated. We not only think that these seasonal signals are supported by our validation but also that the discussion of the seasonal dynamics of the coastal pCO_2 is very relevant to the manuscript and the wider research community. We agree however that the original abstract was not specific enough (especially with respect to seasonal variability) and we will make sure that the updated abstract better reflects the novelty of our approach.

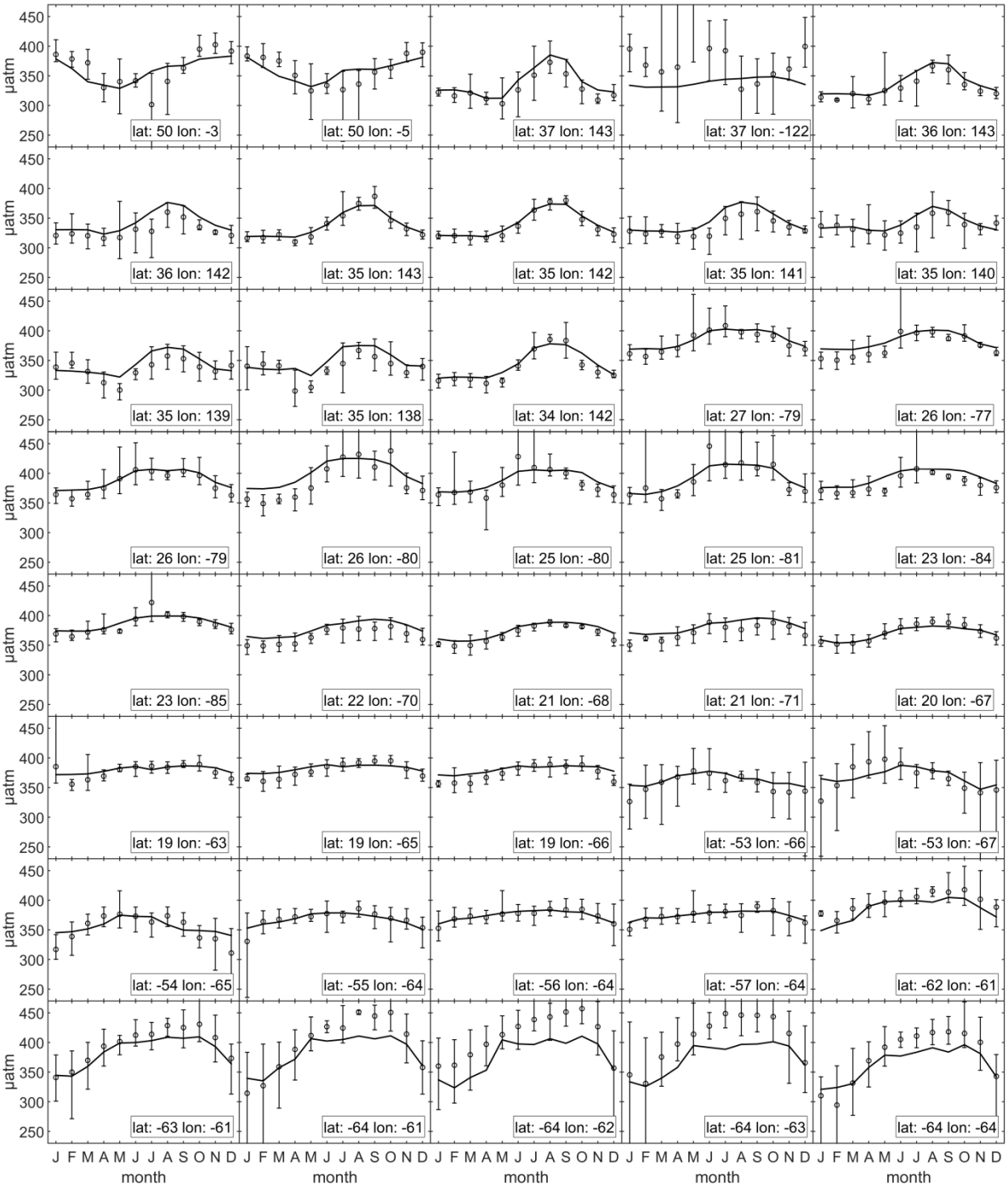

Figure: Climatological monthly mean pCO_2 extracted from the LDEO* database (points) and generated by the artificial neural network (lines) for grid cells having more than 40 months of data. The error bars associated with the data represent the inter-annual variability, reported as the highest and lowest recorded values for a given month at a given location.

Line 36-39, "Overall, the seasonality in shelf pCO2 cannot solely be explained by temperature-induced changes in solubility, but are also the result of seasonal changes in circulation, mixing, and biological productivity."

This should be well known by everybody. I wonder what it adds to place this sentence in the abstract. It is not clear if it is to explain the seasonality the model produced is not satisfied, or simply to explain the seasonality. One may guess that in the model only temperature was included, so the modeling seasonality can't be explained. But in fact salinity, chlorophyll and sea-ice were all included as predictors in the model, with circulation, mixing, and biological productivity all considered in addition to temperatureinduced changes in solubility.

[5] We agree with the reviewer that all readers familiar with the dynamics of carbon in coastal waters will be aware that the seasonal changes of pCO_2 are not only driven by temperature variations but also hydrodynamics, planktonic productivity etc... The purpose of this sentence was to refer to our analysis of the effect of temperature change on the seasonal cycle of pCO_2 presented at the end of section 3 but we agree that the phrasing was too generic and did not report any new finding. In the updated manuscript, the abstract will be more specific and the outcome of our seasonal analysis more clearly presented (i.e. in which regions of the world, is temperature the dominant driver of the seasonal change in coastal pCO_2, see also answer [4]).

Line 118, it is Landschützer et al. 2015? Should it be 2014?
[6] Indeed, the SOM FFN method is only briefly described in Landschützer et al. (2015) and the reference will be replaced by Landschützer et al. (2014) in the updated manuscript.

Line 141-144, "This approach facilitates future integration with existing global ocean data products (e.g., Landschützer et al., 2016; Rödenbeck et al., 2015) and model outputs, which typically struggle to represent the shallowest parts of the ocean (Bourgeois et al., 2016)". Can you explain what the inner boundary of the global ocean data products is, where they are still confident? I do not think 500 m depth would still be too shallow to struggle. I would think that using 500 m depth as the outer boundary of shelf model would be more than enough (You used 1000 m depth as the outer boundary).
[7] Unfortunately, there is no such thing as a universally accepted inner boundary for ocean data products and models but the extension of their simulation domain varies from one study to the other. The 200m isobaths if commonly used as limit between the open ocean and continental shelves but this limit is somewhat artificial (Walsh et al., 1988, Laruelle et al., 2013). The purpose of extending our outer limit for coastal water as far as 1000m depth is to insure an overlap between coastal and oceanic data product to prevent some regions of the world to remain untreated by either approaches.

Line 152-156, chlorophyll was not included to define biogeochemical provinces using SOM?
[8] Indeed, chlorophyll was not included to define the biogeochemical provinces using SOM, due to the fact that the data coverage is incomplete in the high latitudes in winter due to e.g. cloud coverage. This is the same reason Chl a is excluded from the calculations of provinces P8, P9 and P10 during the Feed Forward Network step. This will be clarified in the text.

Line 185-189, SeaWiFS extends to 2014? Please double-check. To my knowledge, it ends in 2010. By the way, normally people write it as SeaWiFS, not SeaWIFS.

[9] As pointed out by the reviewer, SeaWiFS data do not extend past 2010. The data used later than this date and all the way to December 2015 are taken for MODIS. Also, SeaWiFS will be written as suggested by the reviewer throughout the updated manuscript. This reply will be used to clarify the manuscript and details will be included in the table listing all data sources (see answer [1]).

Line 186, should it be "one of the environmental drivers"?
[10] The sentence will be corrected as suggested.

Section 2.2, it would be better if to appear before the model. Then no need to ask readers to "see below" in Line 164 and 168.
[11] Following the reviewer's suggestion, the sections 2.1 and 2.2 of the manuscript will be inverted, in order to present the datasets used and their processing, before describing the modifications performed to the SOM_FFN.

Line 198, why ice was recalculated? And what kind of recalculation?
[12] The original spatial resolution of the sea ice coverage is days and monthly averages had to be calculated from the original data as well as monthly rates of change in sea ice coverage. This is now explained more clearly in the updated manuscript. In addition, the new table 2 listing all the original spatial and temporal resolutions of all datasets and the manipulations performed with them will help make the data processing more transparent.

Line 211-222 is not evaluation. It is the model training.
[13] Following the reviewer's suggestion, this subsection has been renamed 'model training'.

Line 216, do you mean you used chlorophyll in FFN but not in SOM? Why?
[14] Indeed chlorophyll was used in FFN but not in SOM as justified in answer [8].

I would say that the entire data and method section is really confusing. A cartoon, with input and out clearly indicated, and calibration (training) and validation clearly separated, would help. Also, why twice FFN? The rationale to do this is not clear.

[15] We agree with the reviewer that the different steps and datasets required by our approach may be confusing to the reader and we now improved the clarity of the method in the updated manuscript. In particular, the suggestion of the reviewer to use a conceptual scheme detailing the different steps of the method will be included in the revised ms.
As for the choice of using twice the FFN, it is true that such choice is uncommon and generally not required in a Feedforward Network. Following the remarks of both reviewers regarding this modification, another solution was considered to replace the second neuron layer with the use of a sigmoid activation function bounded between 0 and 1 in the hidden layer. The implementation of this solution did not deteriorate the overall results. The new simulations were thus carried out with this new setting which only uses a single neuron layer.

Line 353-359, this explanation is confusing. There is no reason why results from the global open ocean model can be so different from the coastal model in the overlapped

cells. The only critical changes are higher resolution (actually it is an interpolation) and sea ice. Have you tried giving up ice, let other conditions be the same, see what it will be?

[16] As mentioned in answer [1], we do not agree with the notion that our results are just an interpolation of the oceanic model. Other than the spatial resolution and the choice of environmental predictors, both oceanic and coastal models were trained on fundamentally different datasets – the open ocean model was trained with open ocean pCO_2 measurements and the coastal model was trained with coastal pCO_2 measurements. Therefore, we are not surprised that the 2 estimates differ in overlapping areas. However, we do agree that the magnitude of disagreement is somewhat larger than one would expect, highlighting on the one hand current knowledge gaps regarding the coastal to open ocean continuum and on the other hand that more research is needed to close this knowledge gap. The suggestion from the reviewer to perform simulations without the new coastal predictors to quantify their effect is now also included in the updated manuscript, as already discussed in answer [3].

Fig. 2, suggest to use other color, say brown for lands. It is now not easy to tell ice cover from the land.

[17] The suggestion of the reviewer has been implemented in the new version of the manuscript. As an example, all the maps presented in these replies already use a brown colour to represent land.

Literature cited in the responses:

Cavalieri, D. J., Parkinson, C. L., Gloersen, P., and Zwally, H.: Sea Ice Concentrations from Nimbus-7 SMMR and DMSP SSM/I-SSMIS Passive Microwave Data, years 1990–2011, NASA DAAC at the Natl. Snow and Ice Data Cent., Boulder, Colo. (Updated yearly.), 1996.

Cooley, S. R., V. J. Coles, A. Subramaniam, and P. L. Yager (2007), Seasonal variations in the Amazon plume-related atmospheric carbon sink, Global Biogeochem. Cycles, 21, GB3014, doi:10.1029/2006GB002831.

Dee, D. P., Uppala, S. M., Simmons, A. J., Berrisford, P., Poli, P., Kobayashi, S., Andrae, U., Balmaseda, M. A., Balsamo, G., Bauer, P., Bechtold, P., Beljaars, A. C. M., van de Berg, L., Bidlot, J., Bormann, N., Delsol, C., Dragani, R., Fuentes, M., Geer, A. J., Haimberger, L., Healy, S. B., Hersbach, H., Hòlm, E. V., Isaksen, L., Kallberg, P., Köhler, M., Matricardi, M., Mcnally, A. P., Monge-Sanz, B. M., Morcrette, J. J., Park, B. K., Peubey, C., de Rosnay, P., Tavolato, C., Thépaut, J. N. and Vitart, F.: The ERA-Interim reanalysis: Configuration and performance of the data assimilation system, Q. J. R. Meteorol. Soc., 137(656), 553–597, doi:10.1002/qj.828, 2011.

Good, S. A., M. J. Martin and N. A. Rayner, 2013. EN4: quality controlled ocean temperature and salinity profiles and monthly objective analyses with uncertainty estimates, Journal of Geophysical Research: Oceans, 118, 6704-6716, doi:10.1002/2013JC009067

Ibánhez, J. S. P., D. Diverrès, M. Araujo, and N. Lefèvre (2015), Seasonal and interannual variability of sea-air CO2 fluxes in the tropical Atlantic affected by the Amazon River plume, Global Biogeochem. Cycles, 29, 1640–1655, doi:10.1002/2015GB005110.

Landschützer, P., Gruber, N., Bakker, D. C. E., Schuster, U., Nakaoka, S., Payne, M. R., Sasse, T., and Zeng, J.: A neural network-based estimate of the seasonal to inter-annual variability of the Atlantic Ocean carbon sink, Biogeosciences, 10, 7793-7815, doi:10.5194/bg-10-7793-2013, 2013.

Landschützer, P., Gruber, N., Bakker, D. C. E., and Schuster, U.: Recent variability of the global ocean carbon sink, Global Biogeochemical Cycles, 28, 927–949, doi:10.1002/2014GB004853, 2014.

Landschützer, P., Gruber, N., Haumann, F. A. Rödenbeck, C. Bakker, D.C.E. , van Heuven, S. Hoppema, M., Metzl, N., Sweeney, C., Takahashi, T., Tilbrook, B. and Wanninkhof, R.: The reinvigoration of the Southern Ocean carbon sink, Science, 349, 1221-1224. doi: 10.1126/science.aab2620, 2015.

Laruelle, G. G., Dürr, H. H., Lauerwald, R., Hartmann, J., Slomp, C. P., Goossens, N., and Regnier, P. A. G.: Global multi-scale segmentation of continental and coastal waters from the watersheds to the continental margins, Hydrol. Earth Syst. Sci., 17, 2029-2051, doi:10.5194/hess-17-2029-2013, 2013.

NASA Goddard Space Flight Center, Ocean Ecology Laboratory, Ocean Biology Processing Group; (Dataset Release 2016): MODIS-Aqua chlorophyll Data; NASA Goddard Space Flight Center, Ocean Ecology Laboratory, Ocean Biology Processing Group, 2016.

U.S. Department of Commerce, National Oceanic and Atmospheric Administration, National Geophysical Data Center. 2006. 2-minute Gridded Global Relief Data (ETOPO2v2). http://www.ngdc.noaa.gov/mgg/fliers/06mgg01.html. Accessed 21 May 2017.

Walsh, J. J.: On the nature of continental shelves, Academic Press, San Diego, New York, Berkeley, Boston, London, Sydney, Tokyo, Toronto, 1988.

Global high resolution monthly pCO_2 climatology for the coastal ocean derived from neural network interpolation

Running head: Global coastal pCO_2 maps

Goulven G. Laruelle[1], Peter Landschützer[2], Nicolas Gruber[3], Jean-Louis Tison[1], Bruno Delille[4], Pierre Regnier[1]

1. Department Geoscience, Environment & Society (DGES), Université Libre de Bruxelles, Belgium
2. Max Planck Institute for Meteorology, Hamburg, Germany
3. Environmental Physics, Institute of Biogeochemistry and Pollutant Dynamics, ETH Zürich, Zürich, Switzerland
4. Unité d'Oceanographie Chimique, Astrophysics, Geophysics and Oceanography department, University of Liège, Belgium

Corresponding author: Goulven G. Laruelle

Revised version of manuscript bg-2017-64 (Minor revisions)

Deleted: For submission to Biogeosciences

Abstract

In spite of the recent strong increase in the number of measurements of the partial pressure of CO_2 in the surface ocean (pCO_2), the air-sea CO_2 balance of the continental shelf seas remains poorly quantified. This is a consequence of these regions remaining strongly under-sampled both in time and space, and of surface pCO_2 exhibiting much higher temporal and spatial variability in these regions compared to the open ocean. Here, we use a modified version of a two-step artificial neural network method (SOM-FFN, Landschützer et al., 2013) to interpolate the pCO_2 data along the continental margins with a spatial resolution of 0.25 degrees and with monthly resolution from 1998 until 2015. The most important modifications compared to the original SOM-FFN method are (i) the much higher spatial resolution, and (ii) the inclusion of sea-ice and wind speed as predictors of pCO_2. The SOM-FFN is first trained with pCO_2 measurements extracted from the SOCATv4.0 data base. Then, the validity of our interpolation, both in space and time, is assessed by comparing the generated pCO_2 field with independent data extracted from the LDVEO2015 data base. The new coastal pCO_2 product confirms a previously suggested general meridional trend of the annual mean pCO_2 in all the continental shelves with high values in the tropics and dropping to values beneath those of the atmosphere at higher latitudes. The monthly resolution of our data product permits us to reveal significant differences in the seasonality of pCO_2 across the ocean basins. The shelves of the western and northern Pacific, as well as the shelves in the temperate North Atlantic display particularly pronounced seasonal variations in pCO_2, while the shelves in the southeastern Atlantic and in the South Pacific reveal a much smaller seasonality. The calculation of temperature normalized pCO_2 for several latitudes in different oceanic basins confirms that the seasonality in shelf pCO_2 cannot solely be explained by

Deleted: 4

Deleted: a

Deleted: The validity of our interpolation, both in space and time, is assessed by comparing the SOM-FFN outputs

Deleted: SOCATv3

Formatted: Subscript

Deleted: and

Deleted: LDVEO2014

Deleted: sets

Deleted: But

Deleted: allows investigating the seasonal variations in pCO_2 and reveals

Formatted: Subscript

Formatted: Subscript

Deleted: exist

Deleted: Overall

Deleted: cycles

Deleted: ,

Formatted: Subscript

temperature-induced changes in solubility, but are also the result of seasonal changes in circulation, mixing, and biological productivity. Our results also reveal that the amplitudes of both thermal and non-thermal seasonal variations in pCO_2 are significantly larger at high latitudes. Finally, thanks to this product having been extended to cover open ocean areas as well, it can be readily merged with existing global open ocean products to produce a true global perspective of the spatial and temporal variability of surface ocean pCO_2.

Formatted: Subscript

Formatted: Not Superscript/ Subscript

1. Introduction

The quantitative contribution of the coastal ocean to the global oceanic uptake of atmospheric CO_2 is still being debated (Borges et al., 2005; Chen and Borges, 2009; Cai, 2011; Wanninkhof et al., 2013; Gruber, 2015), but several recent studies have suggested that the flux density, or uptake per unit area, is greater over continental shelf seas than over the open ocean (Chen et al., 2013; Laruelle et al., 2014). Laruelle et al. (2014) used more than $3 \cdot 10^6$ pCO_2 measurements from the SOCATv2 database (Pfeil et al., 2014 Bakker et al., 2016) to demonstrate very strong disparities in air-seawater CO_2 exchange at the regional scale as well as pronounced seasonal variations, especially at temperate latitudes. Furthermore, it was suggested that, despite the presence of a seasonally varying sea-ice cover, Arctic continental shelves are a regional hotspot of CO_2 uptake (Bates et al., 2006; Laruelle et al., 2014; Yasunaka et al., 2016). Yet, even with this much larger dataset compared to previous studies, large regions of the global coastal ocean remained either void of data or very poorly monitored in space and time, including the seasonal cycle. These data gaps not only limit our ability to reduce uncertainties in flux estimates and to unravel whether they differ from the adjacent open ocean, but also hamper the identification and quantification of the many processes controlling the source-sink nature of the coastal ocean (Bauer et al., 2013). Laruelle et al., (2014) attempted to overcome this limitation by combining various upscaling methods depending on data density in different regions, e.g., resorted to using annual means, wherever the seasonal coverage was deemed to be insufficient. But they could not overcome the limitation that the data alone are insufficient to assess whether there are any trends in coastal fluxes. This is a serious gap when considering that the influence of human activity on coastal system is increasing rapidly (Doney, 2010; Cai, 2011; Regnier et al., 2013; Gruber, 2015).

Deleted: reports

Deleted: de

Deleted: do

Deleted: underlying

In the open ocean, novel statistical methods relying on artificial neural networks (ANNs) have permitted the generation of a series of high-resolution continuous monthly maps for ocean surface CO_2 partial pressures (pCO_2) (e.g., Landschützer et al., 2013; Sasse et al., 2013; Nakaoka et al., 2013; Zeng et al., 2014). Although differing in their details (see e.g., Rödenbeck et al., 2015 for an overview), these products typically have a nominal spatial resolution of 1-degree and monthly temporal resolution. By filling in the spatial and temporal gaps, these products greatly facilitate the calculation of the air-sea CO_2 exchange, as they do not require separate assumptions about the surface ocean pCO_2 in areas lacking data. Such methods are also well suited to resolve spatial gradients, and they also permit to determine seasonal and inter-annual variations and trends in pCO_2 (e.g., Landschützer et al., 2014, 2015, 2016; Zeng et al., 2014). Because of the small relative contribution of the coastal ocean to the total oceanic surface area and the relatively coarse spatial resolution of the ANN-based surface ocean pCO_2 products so far, they are not well suited to resolve the high spatio-temporal variations of the surface ocean pCO_2 fields along the shelves.

Reproducing the complex seasonal dynamics of the CO_2 exchange at the air-water interface in the coastal ocean is of particular importance considering that they often have large intra-annual variability (Signorini et al., 2013). For instance, in temperate climates, it is common for continental shelf waters to turn from CO_2 sinks for the atmosphere during spring to CO_2 sources during summer (Shadwick et al., 2010; Cai, 2011; Laruelle et al., 2014, 2015). Shelf waters are also typically characterized by small-scale physical features such as coastal currents, river plumes and eddies inducing sharp biogeochemical fronts (Liu et al., 2010) that markedly influence the spatial patterns of the pCO_2 fields (e.g., Turi et al., 2014).

Deleted: have

Deleted: display

To resolve the high spatial and temporal variability in air-sea CO_2 exchange over the global shelf region, the two step artificial neural network method developed by Landschützer et al. (2013) is modified here for the specific conditions that prevail in these environments. Our calculations are performed at a much finer resolution of 0.25 degree and new environmental drivers such as sea ice cover are used at high latitudes to account for the potentially significant role of sea-ice in the CO_2 exchange (Bates et al., 2006; Vancoppenolle et al., 2013; Parmentier et al., 2013; Moreau et al., 2016; Grimm et al., 2016). The definition of the coastal/open oceanic boundary varies strongly from one study to the other (Walsh, 1988; Laruelle et al., 2013), with a potentially large impact on the shelf CO_2 budget (Laruelle et al., 2010). Here, we use a very wide definition for this boundary (i.e., 300km width or 1000m depth) to secure spatial continuity between our new shelf pCO_2 product and those already existing for the open ocean (Landschützer et al., 2013, 2016; Rödenbeck et al., 2015). Our approach leads to the first continuous and monthly resolved pCO_2 maps over the 1998-2015 period across the global shelf region, permitting us to study the seasonal dynamics of these regions in relationship to that of the adjacent open ocean.

Deleted: significantly

Deleted: climatology

Deleted: (

Deleted: 4

Deleted:)

2. Methods

The method used in this study is a modified version of the SOM-FFN method developed by Landschützer et al. (2013) to calculate monthly-resolved pCO_2 maps of the Atlantic Ocean at a 1 degree resolution and later applied to the entire global open ocean (Landschützer et al., 2014). The reconstruction of a continuous pCO_2 field involves establishing numerical relationships between pCO_2 and a number of independent environmental predictors that are known to control its variability both in time and space. The first step of the method relies on

the use of a neural network clustering algorithm (Self Organizing Map, SOM) to define a discrete set of biogeochemical provinces characterized by similar relationships between the independent environmental variables and a monthly resolved pCO_2 field. The second step consists in deriving non-linear and continuous relationships between pCO_2 and some or all of the aforementioned independent variables using a feed-forward network (FFN) method, within each biogeochemical province created by the SOM. The method is extensively documented in Landschützer et al. (2013, 2014) but the specific modifications introduced in this study to better simulate the characteristics of the shelves, the choice of environmental drivers and their data sources as well as the definition of the geographic extent of this analysis are described in the following sections. Figure 1 summarizes the different steps involved in the calculations of the SOM-FFN.

2.1. Data Sources and processing

All the datasets used in our calculations were converted from their original spatial resolutions to a regular 0.25 degree resolution grid. The temporal resolution of all datasets is monthly (i.e., 216 months over the entire period), except for the bathymetry that is assumed constant over the course of the simulations and wind speed whose original resolution is 6 hours. For the latter, monthly averages are calculated for each grid cell to generate monthly values. SST and SSS maps were taken from the Met Office's EN4, which consists of quality controlled subsurface ocean temperature and salinity profiles and their objective analyses (Good et al., 2009). The bathymetry was extracted from the global ETOPO2 database (US Department of Commerce, 2006). The sea ice concentrations was taken from the global 25 km resolution monthly data product compiled by the NSIDC (National Snow and Ice Cover Data; Cavalieri

Deleted: climatological

Deleted: described

Deleted: 2015

Formatted: Not Highlight

Moved (insertion) [1]

Deleted: 2

Deleted: 04

Deleted: which

Deleted: :

Deleted: World Ocean Atlas (Antonov et al., 2010 for SST and Locarnini et al., 2010 for SSS)

Deleted: are

Deleted: recalculated

Deleted: extracted

et al., 1996). Wind speed data were extracted from ERA-Interim reanalysis (Dee et al., 2011). The chlorophyll surface concentrations were extracted from the monthly 9 km resolution SeaWIFS data product prior to 2010 and from MODIS for later years (NASA, 2016). The list of all data products used in the calculations as well as the transformations applied to produce monthly 0.25 degrees resolution forcing files are summarized in table 1.

Finally, the surface ocean pCO_2 were taken from the gridded SOCATv4 product (Sabine et al., 2013; Bakker et al., 2016) while those used for the validation stem from the LDEOv2015 database (Takahashi et al., 2016). With our definition of the coastal zone, SOCATv4 contains ~8 10^6 data points and LDEO ~5.6 10^6, with over 70% of the data shared with SOCATv4. Because of this significant overlap between both data products, we created two entirely independent datasets by randomly assigning each of those common data point to either database to insure that each data only belongs to one dataset. The resulting datasets are named SOCAT* and LDEO*, respectively, with the former being used for training and the latter for validation. Prior to the creation of both datasets, all data from SOCAT were converted from fCO_2 (fugacity of CO_2 in water) to pCO_2 using the formulation reported in Takahashi et al. (2012). The data densities of SOCAT* and LDEO* are shown on Fig. 2 and reveal a heterogeneous spatial coverage. Northern temperate shelves are generally well covered, especially in the North Atlantic. In this region, the data density is better in SOCAT* than LDEO* thanks to the addition of many European cruises in the SOCAT database. On the other hand, equatorial regions remain under-sampled, especially in the Indian Ocean. Because of the difficulty of sampling in waters seasonally covered in ice, Polar Regions are very unevenly represented in SOCAT* and LDEO*. Luckily, some areas, such as some parts of

Deleted: 3

Deleted: r

Deleted: m

Deleted: are extracted

Deleted: v2014

Deleted: However

Deleted: under

Formatted: Font: 12 pt

Formatted: Font: 12 pt

Deleted: of which are also part of

Formatted: Font: 12 pt, Superscript

Formatted: Font: 12 pt

Formatted: Font: 12 pt, Superscript

Formatted: Font: 12 pt

Deleted:

Formatted: Font: 12 pt

Formatted: Font: 12 pt

Formatted: Font: 12 pt

Deleted: ed

Formatted: Font: 12 pt

Deleted: were

Deleted: which was used for calibration and

Deleted: which was used

Deleted: in

Deleted: overall

Antarctica and the Bering Sea do contain enough data to train and validate the SOM-FFN. Overall SOCAT* contains roughly 40% more data than LDEO*.

2.2. Modifications of the SOM-FFN method

The specific characteristics of the continental shelves motivated a number of modifications of the global ocean SOM-FFN method, including a 16-fold increase in spatial resolution from 1 degree to 0.25 degree, the addition of new environmental variables as biogeochemical predictors, and a shortening of the simulation period to the period 1998 through 2015. All these modifications are detailed here below.

The higher resolution of 0.25°×0.25° results in over 2 million grid cells that help to better track the global coastline and its complex geomorphological features (Crossland et al., 2005; Liu, 2010). It is also common along Eastern and Western boundary currents to find continental shelves as narrow as 10-20 km, i.e., an extension that is significantly smaller than a single cell at 1-degree resolution. Additionally, biogeochemical fronts associated with river plumes, coastal currents and upwelling are characterized by spatial scales of the order of tens of kilometers or even smaller (Wijesekera et al., 2003). The chosen resolution is also identical to the gridded coastal pCO_2 product from the SOCAT initiative (Sabine et al, 2013, Bakker et al., 2014).

The definition of the geographic extent of the shelf region excludes estuaries and other inland water bodies, but uses a wide limit for the outer continental shelf that encapsulates all current definitions of the coastal ocean. This approach facilitates future integration with existing global ocean data products (e.g., Landschützer et al., 2016; Rödenbeck et al., 2015) and model outputs, which typically struggle to represent the shallowest parts of the ocean

Deleted: calibrate

Deleted: This latter database contains ~ 10.5 million pCO_2 measurements collected between 1957 and 2015. While a large overlap with the SOCAT database is inevitable, LDEOv2014 was compiled independently and is the only other global pCO_2 dataset (of comparable size and coverage to SOCAT) presently available. The data from SOCAT were converted from fCO_2 (fugacity of CO_2 in water) into pCO_2 using the formulation reported in Takahashi et al. (2012).

Formatted: Font: Not Bold

Deleted: 1

Deleted:

Deleted: the introduction of a second neuron layer in the FFN calculations,

Deleted: 2014

Deleted: in

Deleted: ing

Deleted: thus

Deleted: to

(Bourgeois et al., 2016). The outer limit used here is given by whichever point is the furthest from the coast: either 300 km distance from the coastline (which roughly corresponds to the outer edge of territorial waters (Crossland et al., 2005)) or the 1000 m isobaths (Laruelle et al., 2013). The resulting domain (Fig SI B) covers 77 million km^2, more than twice the surface area generally attributed to the coastal ocean (Walsh et al., 1998; Liu et al., 2010; Laruelle et al., 2013).

The predictor variables for the SOM-FFN networks were chosen based on a set of trial-and-error experiments with the selection criteria being the quality of fit, i.e., the best reconstruction of the available observations. The first step of the SOM-FFN calculations, i.e., the self-organizing map-based clustering (SOM) relies on the assignment of the surface ocean data to biogeochemical provinces sharing common spatio-temporal patterns of sea-surface temperature (SST), sea-surface salinity (SSS), bathymetry, rate of change in sea ice coverage, wind speed and observed pCO_2. Chlorophyll a is not included in the list of environmental factors used to generate the biogeochemical provinces because of the incomplete data coverage at high latitude in winter due to cloud coverage. Both the use of wind speed and the rate of change in monthly sea ice concentration are novelties compared to the set-up of Landschützer et al. (2013). The latter is calculated from the gridded monthly sea ice concentration field of Cavalieri et al. (1996). It allows accounting for the complex processes occurring in melting and forming sea ice that are known to strongly influence the dynamics of the carbon within sea-ice covered areas (Parmentier et al., 2013). This first step is performed without any data normalization of the datasets, as this permits us to give more weight to the pCO_2 data. Based on a series of simulations using different numbers of biogeochemical provinces, we found that a clustering of the data into 10 biogeochemical provinces minimized

Deleted: 1

Deleted:

Deleted:

Deleted: The

Deleted: is a

Deleted: novelty

Deleted: and

Formatted: Subscript

294 the average deviation between simulated and observed pCO_2 (see below) while insuring that
295 at least 1000 different grid cells can be used for validation against LDEO* in each province.
296 In the second step of the estimation procedure, i.e., the application of the feed-forward
297 network method (FFN), SST, SSS, bathymetry, sea-ice concentration and chlorophyll a are
298 used as predictors to establish the non-linear relationships between these predictors and the
299 target pCO_2 (for data sources, see below). Similar to the SOM in step one, the selected
300 variables not only comprise proxies representing the solubility and biological pumps of the
301 coastal ocean, but also yield the best fit to the data. These calculations are done iteratively
302 using a sigmoid activation function on an incomplete dataset in order to perform an
303 assessment on the remaining data after each iteration, until an optimal relationship is found.
304 Additionally, as performed in Landschützer et al. (2015), the output pCO_2 data were smoothed
305 using the spatial and temporal mean of each point's neighboring pixels both in time and space
306 within the 3 pixel neighborhood domain. This operation is performed iteratively and does not
307 significantly alter the results, but it ensures smoother transitions in the pCO_2 field at the
308 boundaries between the provinces. This smoothing method yielded good results for the open
309 Southern Ocean where marked pCO_2 fronts are also observed (Landschützer et al., 2015) and
310 was deemed relevant here due to the potentially strong pCO_2 gradients characterizing the
311 shelves.
312 Another change from the most recent global ocean SOM-FFN application (Landschützer
313 et al., 2016) is the different temporal extension of the simulation period, which covers the
314 period from 1998 through 2015, instead of 1982 through 2011. This overall shortening was
315 necessary because one of environmental driver, i.e., chlorophyll data derived from SeaWIFS,
316 only starts in September 1997 (NASA, 2016). Monthly chlorophyll data throughout the entire

Deleted: During

Deleted: calculation

Deleted: This step now includes a second artificial neuron layer that consists, for each iteration, of an additional procedure of optimization of the relationship fitting. This addition significantly increases the calculation time but prevents the SOM-FFN from generating negative values.

Deleted: 2014

Deleted: only

Deleted: the

simulation period was preferred here over the use of a monthly climatology as done in Landschützer et al. (2016) to better capture inter-annual variability. At the same time, we have been able to extend the coastal product by 4 years to the end of 2015.

2.3. Model training and evaluation

We evaluated the coastal SOM-FFN product using the root mean squared error (RMSE) metric, calculated as the difference between estimated and observed pCO_2. During the early development stage, preliminary simulations were performed using only data from SOCAT v2.0 (Pfeil et al., 2013, Sabine et al. 2013) to train the FFN algorithm. Each simulation was carried out using different subsets of environmental predictors extracted from the complete set (SST, SSS, bathymetry, sea ice concentration and chlorophyll a). The results obtained were then compared to the more complete dataset of SOCAT*, which contain 40% more shelf pCO_2 measurements from 1998 through 2015 (Bakker et al., 2016). This process allowed, for each province, to calculate the RMSE for several combinations of independent predictor variables for the pCO_2. Next, the combinations of predictors displaying the lowest RMSE were kept for the final simulations, which then used all data from SOCAT*. Thus, the pCO_2 calculations in each province potentially rely on a different set of predictors (Table 1).

The coastal SOM-FFN results are validated through a comparison with the LDEO* dataset through the calculation of residuals and RMSE. Additionally, a model-to-model comparison is also performed with the global ocean results of Landschützer et al. (2016) in the regions where the domains overlap. To perform this latter analysis, the coastal high resolution coastal pCO_2 product generated here was aggregated to a regular monthly 1° resolution to match the grid used by Landschützer et al. (2016).

Deleted: ¶

Moved up [1]: 2.2. Data Sources and processing¶

All the datasets used in our calculations were converted from their original spatial resolutions to a regular 0.25 degree resolution grid. The temporal resolution of all datasets is monthly (i.e., 204 months over the entire period), except for the bathymetry that is assumed constant over the course of the simulations. SST and SSS maps were taken from the World Ocean Atlas (Antonov et al., 2010 for SST and Locarnini et al., 2010 for SSS). The bathymetry was extracted from the global ETOPO2 database (US Department of Commerce, 2006). The sea ice concentrations are recalculated from the global 25 km resolution monthly data product compiled by the NSIDC (National Snow and Ice Cover Data; Cavalieri et al., 1996). The chlorophyll surface concentrations were extracted from the monthly 9 km resolution SeaWIFS data product (NASA, 2016). Finally, the surface ocean pCO_2 were taken from the gridded SOCATv3 product (Sabine et al., 2013; Bakker et al., 2016) while those used from the validation are extracted from the LDEOv2014 database (Takahashi et al., 2016). This latter database contains ~ 10.5 million pCO_2 measurements collected between 1957 and 2015. While a large overlap with the SOCAT database is inevitable, LDEOv2014 was compiled independently and is the only other globa[1] ...

Deleted: .¶

¶

Deleted: Evaluation procedures

Deleted: v3.0

Deleted: 2014

Deleted: v3.0

Deleted: v2014

Deleted: base (Takahashi et al., 2016)

Finally, the ability of the coastal SOM-FFN to capture seasonal variations is assessed by comparing the cell-average simulated monthly pCO_2 to monthly means for cells extracted from the LDEO* database. The cells retained for this analysis are all those for which the average for each month could be calculated from measurements performed on at least three different years.

3. Results and discussion

3.1. Biogeochemical provinces

Despite the fact that the SOM is not given any prior knowledge regarding space and time, the spatial distribution of the 10 biogeochemical provinces is mostly controlled by latitudinal gradients and distance from the coast (Figure 3; high-resolution monthly maps are also available in the supplementary information (SI)). Although the exact spatial extent of each province varies from one month to the other following the seasonal variations of the environmental forcing parameters, each province roughly corresponds to one type of climatological setting. Nevertheless, because of these spatial migrations, most cells belong to different provinces depending on the month (see figure SI B). These seasonal migrations are mostly driven by changes in temperature, sea-ice cover, pCO_2 and, to a lesser degree, salinity. P1, P2 (Province 1, etc.) and P4 are three of the largest provinces, covering a total of $35.7 \cdot 10^6$ km^2 and representing warm tropical regions with bottoms at shallow to intermediate depths. During summer, the spatial coverage of P4 expands north- and southward as a consequence of warming. P2 represents tropical regions with deeper bottom depths. P1 and P2 display less seasonal changes in their spatial distribution than P4 due to weaker seasonal temperature changes. P3 and P6, which cover a combined $9.2 \cdot 10^6$ km^2, are found in the Southern

Deleted: v2014

Deleted: 1

Deleted: 1 of

Deleted: and

Formatted: Subscript

Deleted: P1

Deleted: 2

Deleted: the two

Deleted: 26.1

Deleted: 1

Deleted: 3

Deleted: and P4

Deleted: They

Deleted: 1

Deleted: P5

Hemisphere and correspond to sub-polar and temperate regions, respectively. Their spatial distributions are subject to marked latitudinal migrations throughout the year as a result of the large amplitude changes in seasonal temperature observed in mid-latitude coastal waters (Laruelle et al., 2014). Similarly, P7, correspond to temperate Northern Hemisphere waters and display marked seasonal changes including the shelves of the Norwegian basin in summer and most of the Mediterranean Sea in winter. P5, P8, P9 and P10 together cover 22.7·10^6 km^2. These provinces are partly (seasonally) covered by sea-ice with an average spatial ice cover over the study period of 57%, 39%, 54% and 46% for P5, P8, P9 and P10, respectively. P5 represents the shelves of Antarctica all year round. P8 includes large fractions of the enclosed seas at higher northern latitudes such as the Baltic Sea and Hudson Bay while P9 (only 2.9·10^6 km^2) represents permanently deep and cold polar regions. P5 and P10 represent most of the polar shelves (P5 for the Antarctic and P10 for the Arctic) and are covered in sea ice at levels of 57% and 46%, respectively. The regions experiencing most notable shifts in province allocation during the year include the northern Polar Regions as well as the temperate narrow shelves of the Atlantic and Pacific, particularly Western Europe and Eastern North America and Eastern Asia (see Fig. SI B).

3.2. Performance of the coastal SOM-FFN

The mean climatological pCO_2 estimated by the coastal SOM-FFN for annually and seasonally averaged conditions are reported in Figure 3. Before briefly analysing the main spatial and temporal variability of the pCO_2 fields (section 3.3), we evaluate here the overall performance of our interpolation method globally and at the level of each province, including its ability to capture the seasonal cycle.

Deleted: cover a combined 14·10^6 km^2
Deleted: P7,
Deleted: 21.3
Deleted: .1
Deleted: 8.5
Deleted: 41
Deleted: .3
Deleted: 65
Deleted: 5.8
Deleted: P7
Deleted: P10
Deleted: P7
Deleted: P10
Formatted: Not Highlight
Deleted: P8 and P9
Formatted: Not Highlight
Formatted: Not Highlight
Deleted: both the
Formatted: Not Highlight
Deleted: Arctic and
Formatted: Not Highlight
Deleted: 47
Formatted: Not Highlight
Deleted: 56
Formatted: Not Highlight
Deleted: polar regions
Deleted: SI1
Formatted: Not Highlight
Deleted: 2

3.2.1. Comparison with training data (SOCAT*)

Within each province, the pCO_2 simulated by the coastal SOM-FFN are compared to the measurements extracted from SOCAT v4.0 (table 2). Globally, the average difference between observed and simulated pCO_2 is almost null (overall bias = 0.0 µatm) and the absolute bias is lower than 4 µatm in all ten provinces. The average RMSE over all provinces of 32.9 µatm is comparable with those reported for other statistical reconstructions of coastal pCO_2 fields summarized by (Chen et al., 2016), although none of these studies were performed at global scale and many rely on different statistical approaches often using remote sensing data. This RMSE is about twice that achieved for the open ocean (Landschützer et al., 2014) reflecting the larger spatiotemporal variability in the coastal ocean, as well as more complex processes governing that variability. Considering these complexities, achieving at the global scale RMSE in the same range as those reported for regional coastal studies is quite good.

Significant variations in both bias and RMSE can be observed between provinces (table 2). P1 and P3 have the best fit between simulated and observed pCO_2 with RMSE lower than 20 µatm. In 5 provinces that cover a cumulated surface area of 31.2 10^6 km^2 (P1, P2, P3, P6 and P9) RMSE's do not exceed 25 µatm. In P8 however, the maximum RMSE is found with a value of 46.8 µatm. Overall, the performance of the SOM-FFN deteriorates for provinces regularly covered by sea-ice ice (P5, P8-10) in which data coverage is relatively low (RMSE> 34 µatm). This trend is consistent with the spatial distribution of the average residual errors between the pCO_2 field generated by the model and pCO_2 data extracted SOCAT* (Fig. 4a). The residuals are obtained by subtracting the observed values from model output in each grid cell for every month where observations are available. Thus, positive values correspond to cells where the simulated pCO_2 overestimates the field data, while negative values represent

Deleted: SOCAT*
Deleted: v3.0 data
Deleted: 3
Deleted: +
Deleted: 1
Deleted: 6
Deleted:
Deleted: (Chen et al., 2016)
Deleted: the
Deleted: ed
Deleted: P2
Deleted: absolute bias and
Deleted: 2 µatm and
Deleted: , respectively
Deleted: 6
Deleted: which
Deleted: 52
Deleted: .6
Deleted: P4,
Deleted: P8
Deleted: 30
Deleted: P7
Deleted: bias and
Deleted: are maximum
Deleted: s
Deleted: 7.4 µatm and 63.4
Deleted: , respectively
Deleted: P7
Deleted: and
Deleted: and in which R
Formatted: Not Highlight
Formatted: Not Highlight
Formatted: Subscript
Formatted: Subscript

cells where the simulated pCO_2 underestimates the field data. The bulk of the residuals fall in the -20 to 20 µatm range in temperate and tropical regions, except for very shallow regions tha are under the influence of a large river such as the Mississippi. There, the SOM-FFN often underestimates the observed pCO_2. There also exist coastal areas where the SOM-FFN underestimates the observed pCO_2 such as the Nova Scotia, the South Western coast of England or the shelves of California and Morocco. The complex hydrodynamics of those regions (some of them being characterized as upwelling regions) may explain the weaker performance of the SOM-FFN. At high latitudes, the performance of the model deteriorates somewhat. For example, the Bering Sea both contains cells with very high (>50 µatm) and very low average residuals (<-50 µatm).

3.2.2. Evaluation with LDEO* data

The comparison of our results with the data from LDEO* yields a global bias of 0.0 µatm (calculated as the average difference between observed and SOM-FFN estimated pCO_2) for the entire shelf domain. However, the spread is relatively large with an average RMSE of 39.2 µatm. This average RMSE is 19% larger than the one obtained when comparing the SOM-FFN results with the SOCAT* dataset, which has been used to train the model. A province-based analysis reveals strong differences in the calculated RMSEs, ranging from 20 µatm to 53 µatm (Table 2, LDEO*). A review of various statistical models used to generate continuous global ocean pCO_2 maps, including some using remote sensing data and algorithms, reports RMSE or uncertainties typically varying within the 10-35 µatm range (Chen et al., 2016) with outliers as high as 50 µatm in the Mississippi delta (Lohrenz and Cai, 2006). This report also shows that open ocean estimates generally yields RMSE lower than 17

Deleted: cells
Deleted: where
Formatted: Not Highlight
Formatted: Not Highlight
Deleted:
Formatted: Subscript, Not Highlight
Formatted: Not Highlight
Formatted: Subscript
Deleted: r
Deleted: s
Deleted: .
Deleted: and
Deleted: f
Deleted: r
Deleted: hith
Deleted: Comparison
Deleted: v2014
Deleted: v2014
Deleted: very small
Deleted: -2.4
Deleted: 42
Deleted: 24
Deleted: 67

µatm, in agreement with Landschützer et al. (2014), whereas coastal estimates are associated with much higher uncertainties. This is likely because these coastal regions have complex biogeochemical dynamics and high frequency variability that cannot be fully captured with the current generation of data interpolation techniques using the limited available predictor data.

In our simulations, the province averaged biases are larger than those calculated with SOCAT* but their absolute value remains small and never exceed 3.9 µatm (P8). Provinces P1, P2, P3 and P6 have RMSE < 30 µatm, which compares with the most robust pCO_2 regional coastal estimates from the literature (Chen et al., 2016). Together, these 4 provinces account for 37% of our domain. P4, P5 and P9 display RMSE comprised between 33 µatm and 38 µatm for P4 and P9, respectivelly. Overall, these 7 provinces covering the entire tropical and temperate latitudinal bands as well as some subpolar regions account for >72% of the shelf surface area and yield RMSE of less than 38 µatm and absolute biases of less than 2.3 µatm. Provinces in the polar regions (P5, P7, P8 and P10) overall display larger deviations with respect to the LDEO* dataset, but the absolute value of their biases never exceeds 3.9 µatm. Their RMSE all fall in the 51-53 µatm range. This suggests a significantly lower performance of the SOM-FFN in regions partly covered in sea-ice. This can be attributed to the limited number of available data points and their very heterogeneous distribution in time and space, as well as to the very limited range of variation of some of the controlling variable such as temperature and salinity. The relatively good performance of the model in tropical region might be partly attributed to the relatively small seasonal variations in pCO_2 within these areas. The residuals calculated by subtracting the SOM-FFN results from LDEO* are very similar to those obtained by subtracting the SOM-FFN results from SOCAT* (Fig. 4b).

Deleted: integrated
Deleted: provinces
Deleted: P4
Deleted: negligible biases (with absolute values <0.5 µatm, table 2) and
Deleted: 3
Deleted: 44
Deleted: P3
Deleted: P5
Deleted: slightly higher biases of -2.3 and -5.2 µatm, respectively and
Deleted: of
Deleted: 44
Deleted: 67
Deleted: µatm
Deleted: 5
Deleted: 62
Deleted: 45
Deleted: 4
Deleted: sub-polar and
Deleted: P6
Deleted: ,
Deleted: P9
Deleted: v2014
Deleted: 10
Deleted: Except for P8, which displays a
Deleted: of 35 µatm, all other province...
Deleted:
Deleted: ing
Deleted: 45
Deleted: 70
Deleted: s
Deleted: to
Deleted: s
Deleted: to

The residual errors have a nearly Gaussian distribution for every biogeochemical province with the exception of province P8 (Fig. 5). In this case, the distribution has not only the highest spread, but is also skewed toward high values.

In order to evaluate the contribution of the newly added predictors compared to the oceanic set up of the SOM-FFN (Landschützer et al., 2013), the model was also trained without wind speed and sea ice cover. The RMSE obtained with those simulations (Table 4) are significantly higher than those obtained using all predictors (Table 3). However, the overall bias remain small. The results of those simulations are presented in the table below and allow to quantify how the addition of new predictors affects the performance of the model. For instance, it can be noticed that the global RMSE increases significantly (from 39.2 to 48 µatm in the comparison with LDEO* when chlorophyll, sea ice and wind speed are not taken into account and from 39.2 to 45 µatm when only sea ice and wind speed are not taken into account). This deterioration of the performance of the model, however, is not evenly affecting all provinces. Provinces located at high latitudes (i.e. P8, P9 and P10) perform significantly worse without the inclusion of wind speed and sea ice.

Finally, while the use of residuals and RMSE provide valid quantitative assessment of the model performance, it does not provide insights regarding its ability to reproduce the seasonal pCO_2 cycle. To address this issue, Figure 7 displays observed mean monthly pCO_2 extracted from LDEO* and calculated by the coastal SOM-FFN for the 40 locations where the LDEO* database has the most data (>40 month). The error bars associated with the observations reflect the inter-annual variability. Overall, the coastal SOM-FFN captures the timing of the seasonal pCO_2 cycle in most locations well with pCO_2 minima and maxima occurring at the same time in our results and in the uninterpolated LDEO* data. The pCO_2 maximum

Deleted: distribution of the

Deleted: within each biogeochemical province assumes

Deleted: s

Deleted: of the residuals

Deleted: for which the spread is not only the highest (indicating the largest discrepancy between model and observations), but also slightly skewed toward high values, thus revealing a tendency to overestimate the observed pCO_2.

Formatted: Subscript

Deleted: T

Deleted: , however,

Deleted: ing

Deleted: , overall,

Formatted: English (U.S.)

Deleted: s

Deleted: and it can be observed in particular that

Deleted: p

Deleted: ¶

Deleted: W

Deleted: of

Deleted: s

Deleted: a

Deleted: 3

Deleted: v2014

Deleted: 53

Deleted: v2014

Deleted: v2014

Deleted: ¶

generally taking place in early summer is accurately captured by the coastal SOM-FFN. In terms of amplitudes in the pCO_2 signal, the coastal SOM-FFN and the LDEO* data reveal primarily how different the seasonal pCO_2 cycle is from one region to the other, with very low amplitude (<40 µatm) in some sub-tropical areas, amplitudes > 100 µatm at high Northern and Southern latitudes, and sometimes very sharp increases during summer like off the coast of Japan. In most regions, the SOM-FFN-based reconstructions are able to capture these variations and predict seasonal amplitudes comparable to those observed in the data. However, in cells for which the difference between observed and simulated seasonal pCO_2 amplitude is larger than 20%, the coastal SOM-FFN tends to systematically underestimate the amplitude of the seasonal pCO_2 cycle. This limitation of our model might result from the often short time scales associated with the continental influences in near-shore locations, which are not captured by the environmental predictors used in our calculation. It may also be the result of very short-term events that are aliased in our monthly average calculations.

Deleted: the most

Deleted: v2014

Deleted: ,

Deleted: at

Deleted: s

3.2.3. Comparison with global SOM-FFN

The comparison of our coastal SOM-FFN results with those of Landschützer et al. (2016) for the overlapping grid cells (Table 3) reveals significant differences between both interpolated data products with a RMSE between 24 and 32 µatm for most provinces except P7, P9 and P10 (53, 55 and 37 µatm, respectively). These RMSE values are comparable, but slightly lower than those obtained for the comparison with the LDEO* database, in line with those observed with the SOCAT* database. The differences (coastal SOM-FFN minus global SOM-FFN), however, are much larger than those observed between our results and the LDEO* database and highlight the current knowledge gap regarding the mean state and

Deleted: 2

Deleted: 20

Deleted: 37

Deleted: P9

Deleted: and

Deleted: _v2014

Deleted: _v2014

variability of the transition zone. They range from -17.9 to 11.7 µatm from one province to the other but only amount to -0.6 µatm when considering the cells from all provinces at once. The overlaping cells used for the comparison with Landschützer et al. (2016) are mostly located over 100km away from the coastline and therefore the open ocean as well as our new shelf ocean data set are constrained by fairly different data because all the 'shelf' cells from the open ocean data product have a pCO_2 calculated by a model calibrated mostly for conditions representative of the open ocean. Overall, the occurrence of large residuals in the shallowest cells of our calculation domain in our results (Fig. 2) suggest that the very nearshore processes controlling the CO_2 dynamics likely are the most difficult to reproduce at the global scale. However, the added value of performing our simulations at the spatial resolution of 0.25° is exemplified by the ability of our model to capture the plumes of larges rivers such as the Amazon, where pCO_2 is significantly lower than that of the surrounding waters (Cooley et al., 2007; Ibanez et al., 2015).

3.3. Spatial and temporal variability of the coastal pCO_2

3.3.1 Spatial variability

Figure 4a presents the annual average pCO_2 estimated by the coastal SOM-FFN, representing the mean over 1998 through 2015 period (monthly climatological maps are shown in Fig. SI A). High annual mean values of pCO_2, close to or above atmospheric levels, are estimated around the equator up to the tropics. This is consistent with previous studies that identified tropical and equatorial coastal regions as weak CO_2 sources for the atmosphere (Borges et al., 2005; Cai, 2011; Laruelle et al., 2010; 2014). A hotspot of very high pCO_2 emerges from our analysis around the Arabian Peninsula, extending into the eastern Mediterranean Sea as well

Deleted: 6
Deleted: 8
Deleted: 6
Deleted:
Deleted: Our
Deleted: indicate
Deleted: with a global SOM-FFN
Deleted: explified
Deleted: which
Deleted: produces an area located North of its river mouth characterized by
Formatted: Subscript
Deleted: values
Deleted: those
Deleted:
Deleted: 2a
Deleted: 2014
Deleted: 2
Deleted: in the Indian Ocean
Deleted: past the tropic of Cancer

as into the Red Sea and the Persian Gulf. These regions are poorly monitored and it remains difficult to assess if pCO_2 values in excess of 450 µatm are realistic or not, but the limited body of available literature suggests that very high pCO_2 are indeed observed in these regions (Ali, 2008; Omer, 2010). The very high temperature and salinity conditions observed in the Red Sea, in particular, reduce the CO_2 solubility and induce very high pCO_2 conditions. However, these predicted pCO_2 lie outside of the range used for the training of the SOM-FFN (typically 200-450 µatm) and should thus be considered with caution. Along the oceanic coast of the Arabian Peninsula, the SOM-FFN predicts pCO_2 ranging from 365 to 390 µatm all year round and thus does not capture the well-known increase in pCO_2 resulting from the monsoon driven summer upwelling in the region (Sarma, 2003; Takahashi et al., 2009).

In both hemispheres, pCO_2 values in the 325 to 370 µatm range are generally reconstructed at temperate latitudes, i.e., up to 50°N and 50°S, respectively. The northern high latitudes generally have very low pCO_2 values, down to 300 µatm and below, a result that is consistent with the Arctic shelves contributing a large proportion (up to 60%) of the global coastal carbon sink (Bates and Mathis, 2009; Cai, 2011; Laruelle et al., 2014). Several hotspots of pCO_2 with values as high as 450 µatm can be observed nevertheless north of 70°N, most notably along the eastern coast of Siberia in winter (see Fig. SI P), which displays a large zone characterized by $pCO_2 > 400$ µatm centred on the mouth of the Kolyma River. Such high pCO_2 values have been punctually observed in Arctic coastal waters (Anderson et al., 2009) and could result from the discharge of highly oversaturated riverine waters. But, overall, pCO_2 measurements over Siberian shelves are rare. Thus, our results should be considered with caution in this region because of the scarcity of data to train and validate the coastal SOM-FFN. It should also be noted that the vast majority of this high pCO_2 region is covered

Deleted: calibration

Formatted: Subscript

Formatted: Subscript

Formatted: Not Superscript/ Subscript

Deleted: 320

Deleted: 360

Deleted: 3

Deleted: around

Deleted: particularly

by sea ice (Fig. 4b&c) and, although the model estimates pCO_2 values over the entire domain, only ice-free (or partially ice-free) cells will contribute to the CO_2 exchange across the air-sea interface (Bates and Mathis, 2009; Laruelle et al., 2014).

3.3.2. Temporal variability

The reconstructed pCO_2 field is also subject to large seasonal variations (see figures SI P&A). To explore these variations further, Figure 8 reports seasonal-mean latitudinal profiles of pCO_2 for continental shelves neighbouring the Eastern Pacific, Atlantic, Indian and Western Pacific, respectively. The analysis excludes continental shelves at latitudes higher than 65 degrees, because a large fraction of these shelves are seasonally covered by sea ice. The latitudinal pCO_2 profiles reveal that, in most regions, highest and lowest pCO_2 values are observed during the warmest and coldest months, respectively. This trend is particularly pronounced at temperate latitudes where the seasonal pCO_2 amplitude can reach 60µatm and is exemplified by regions such as the western Mediterranean Sea or the eastern coast of America, which become supersaturated in CO_2 compared to the atmosphere during the summer months. However, there are a few other regions, where the lowest pCO_2 is found in the summer, such as the Baltic Sea (Thomas and Schneider, 1999). Around the equator, the magnitude of the seasonal variations in pCO_2 is limited and does not exceed 30 µatm.

Although the general latitudinal trend of the annual mean pCO_2 is similar across all continental shelves, significant differences in the seasonality can be observed across the largest ocean basins. In particular, most of the East Pacific shelves, except for latitudes north of 55°N, display limited seasonal change in pCO_2 (typically below 30 µatm) while the West Pacific shelves have seasonal pCO_2 amplitudes that can exceed 50 µatm in temperate regions and 100 µatm at high latitudes (above 55° N). Along the Atlantic shelves, the seasonal signal

Deleted: 2b

Deleted: 2

Deleted: 3

Deleted: 4

Deleted: T

Deleted: ,

Deleted:

Deleted: however,

Deleted: in

Deleted: the

Deleted: p

Deleted: c

Deleted:

Deleted: 40

Deleted: 60

is more pronounced in the north compared to the south, in agreement with Laruelle et al. (2014). Overall, the North Pacific (north of 55°N) displays the most pronounced seasonal change in pCO_2 with a difference of 80 µatm between summer and winter. In the Indian Ocean, the seasonal dynamics of pCO_2 is partly regulated by seasonal upwelling induced by the Monsoon (Liu et al., 2010). In this basin north the equator, April, May and June are the months having the highest pCO_2 and the seasonal variations do not exceed 30 µatm. In contrast, the seasonal cycle is quite pronounced in the Indian Ocean south of the equator (~50 µatm).

Latitudinal profiles of SST (Fig 8, bottom) are similar in all coastal oceans with minimal seasonal variations around the equator and amplitudes as large as 20°C at temperate latitudes. The comparison between the seasonal pCO_2 and SST profiles allows us to assess the contribution of temperature-induced changes in CO_2 solubility to the seasonal pCO_2 variations in the continental shelf waters. However, other factors such as seasonal upwelling and biological activity also strongly influence coastal pCO_2 and contribute to the complexity of the seasonal pCO_2 profiles. To quantify the effect of temperature on seasonal variations of pCO_2, the latter is normalized to the mean temperature at different latitudes in each oceanic basin (Fig. 8) using the formula proposed by Takahashi et al. (1993):

$$pCO_{2(SSTmean)} = pCO_{2,obs} \times exp\left(0.0423 \times (T_{mean} - T_{obs})\right) \quad (1)$$

where $pCO_{2(SSTmean)}$ is the temperature normalized pCO_2, $pCO_{2,obs}$ is the observed pCO_2 at the observed temperature T_{obs}, and T_{mean} is the yearly mean temperature at the considered location. In sea-water, an increase in water temperature induces a decrease in gas solubility which leads to a higher water pCO_2. Thus, comparing $pCO_{2(SSTmean)}$ with observed pCO_2

Deleted: above
Deleted: displaying
Deleted: 40
Deleted: 60
Deleted: 4
Deleted: and display
Deleted: bility
Deleted: 5
Deleted: *n*
Deleted: $npCO_2$
Formatted: Not Superscript/ Subscript
Deleted: n

monthly values provides a quantitative estimate of the influence of seasonal temperature change on the seasonality of pCO_2.

For most latitudes and oceanic basins, pCO_2 is minimum in late winter or early spring, i.e., at the time when $pCO_{2(SSTmean)}$ has its maximum. pCO_2 also generally displays a maximum in summer, while $pCO_{2(SSTmean)}$ reaches its minimum then (Fig. 9). The amplitude of the changes in $pCO_{2(SSTmean)}$ is quite consistent across oceans and about 2 to 3 times larger than that of pCO_2. Between 45°N and 60° N, the variations in $pCO_{2(SSTmean)}$ largely exceed 100 µatm (up to 220 µatm at 60° N in the West Pacific). In these regions, the magnitude of the seasonal temperature changes is also maximum and reaches 20° C between winter and summer (Fig. 5). A seasonal signal in pCO_2 with a minimum in late winter or spring when $pCO_{2(SSTmean)}$ is maximal can also be identified. However, the magnitude of the seasonal variations in pCO_2 is significantly smaller than those of $pCO_{2(SSTmean)}$, suggesting that other processes such as biological uptake or transport/mixing partly offsets the temperature effect on solubility. In the subpolar western Pacific shelves (60° N), a second pronounced dip in pCO_2 following a weaker one in spring is observed in summer, which suggests the occurrence of a pronounced summer biological activity taking up large amounts of CO_2. This would also explain the sharp increase in pCO_2 in the following month, as a result of the degradation of organic matter synthesized during the summer bloom. Although this region is also the one subjected to the strongest seasonal temperature, the amplitude of the seasonal $pCO_{2(SSTmean)}$ which reaches 220µatm suggests that non thermal processes drive most of the seasonal pCO_2 variations in the regions. At 20° N, the amplitude of the changes in both pCO_2 and $pCO_{2(SSTmean)}$ are lower than at higher latitudes. pCO_2 varies by ~30µatm between summer and winter in all oceanic basin while the seasonal variations in $pCO_{2(SSTmean)}$ are more pronounced in the Pacific

Deleted: all
Formatted: Not Highlight
Deleted: npCO2
Deleted: npCO2
Deleted: 5
Deleted: npCO2
Deleted: npCO2
Deleted: 180
Deleted: 4
Deleted: npCO2
Deleted: npCO2
Deleted: T
Deleted: gradient as evidenced by
Deleted: npCO2
Deleted: 200µatm
Formatted: Subscript
Deleted: npCO2
Deleted: npCO2

941 (~60µatm) than in the Atlantic or the Indian Oceans. In the Southern Hemisphere, the
942 seasonal variations in pCO_2 are not as pronounced as in the Northern Hemisphere suggesting
943 that the changes induced by the solubility pump are compensated by biological activities. At
944 10°S and 30°S, the seasonal variations in pCO_2 rarely exceed 30 µatm in either basin with a
945 minimum observed around August.
946
947 **4. Summary**
948 This study presents the first global high-resolution monthly pCO_2 maps for continental shelf
949 waters at an unprecedented 0.25° spatial resolution. We show that when tailored for the
950 specific conditions of shelf systems, the SOM-FFN method previously employed in the open
951 ocean is capable of reproducing well-known and well-observed features of the pCO_2 field in
952 the coastal ocean. Our continuous shelf product allows, for the first time, to analyze the
953 dominant spatial patterns of pCO_2 across all ocean basins and their seasonality. The data
954 product associated to this manuscript consists of a netcdf file containing the pCO_2 for ice-free
955 cells at a 0.25° spatial resolution for each of the 216 month of the simulation period (from
956 January 1998 to December 2015). 12 maps representing mean pCO_2 fields calculated for each
957 month over the simulation period are also provided. This data product can be combined with
958 wind field products such as ERA-interim (Dee, 2010; Dee et al., 2011) or CCMP (Atlas et al.,
959 2011) to compute spatially and temporally resolved air-sea CO_2 fluxes across the global shelf
960 region, including the Arctic. Maps including pCO_2 for ice covered cells are also available but
961 should be treated with care because the dynamics of CO_2 fluxes through sea ice are still
962 poorly understood and air-sea gas transfer velocities in partially sea ice covered areas cannot
963 be predicted from classical wind speed relationships (Lovely et al. 2015)

Deleted:

Deleted: ,

Deleted: 204

Deleted: 2014

Formatted: Subscript

Deleted: Climatologically averaged pCO_2 maps for each month

5. Data availability

The version 4 of the SOCAT database (Bakker et al., 2016) can be downloaded from www.socat.info/upload/SOCAT_v4.zip. The observation-based global monthly gridded sea surface pCO_2 product is provided by Landschützer, et al. (2015; doi: 10.3334/CDIAC/OTG.SPCO2_1982_2011_ETH_SOM-FFN.), was downloaded from http://cdiac.ornl.gov/ftp/oceans/SPCO2_1982_2011_ETH_SOM_FFN and is now available at: https://www.nodc.noaa.gov/ocads/oceans/SPCO2_1982_2015_ETH_SOM_FFN.html. The LDEOv2015 database (Takahashi et al., 2015; doi: 10.3334/CDIAC/OTG.NDP088(V2015)) was downloaded from http://cdiac.ornl.gov/oceans/LDEO_Underway_Database/. The global atmospheric reanalysis ERA-interim datasets (Dee et al., 2011, http://doi.wiley.com/10.1002/qj.828) are accessible on the European Centre for Medium-Range Weather Forecasts (ECMWF) website. SST and SSS were extracted from the Met Office's EN4 data set (Good et al., 2009; doi:10.1002/2013JC009067). The bathymetry used is the global ETOPO2 database (US Department of Commerce, 2006), which can be downloaded from http://www.ngdc.noaa.gov/mgg/fliers/06mgg01.html. The sea ice concentrations are derived from the global 25 km resolution monthly data product compiled by the NSIDC (National Snow and Ice Cover Data; Cavalieri et al., 1996).

6. Competing interests

The authors declare that they have no conflict of interest.

Formatted: Font: Not Bold
Formatted: Font: Not Bold, Subscript
Formatted: Font: Not Bold
Formatted: Font: Not Bold
Formatted: Font: Not Bold
Formatted: Font: Not Bold
Formatted: Hyperlink, Font: 10,5 pt, Not Bold, English (U.S.)
Field Code Changed
Formatted: Font: Not Bold
Formatted: Font: Not Bold
Formatted: Font: Not Bold
Formatted: Font: Not Bold
Formatted: Not Highlight
Deleted: : quality controlled subsurface ocean temperature and salinity profiles and objective analyses
Formatted: Not Highlight
Formatted: Not Highlight
Formatted: Not Highlight
Formatted: Not Highlight
Formatted: Font: Not Bold
Formatted: Font: Not Bold

Acknowledgements

G. G. Laruelle and B Delille are postdoctoral researcher and research associate, respectively, of F.R.S.-FNRS. The Surface Ocean CO_2 Atlas (SOCAT) is an international effort, supported by the International Ocean Carbon Coordination Project (IOCCP), the Surface Ocean Lower Atmosphere Study (SOLAS), and the Integrated Marine Biogeochemistry and Ecosystem Research program (IMBER), in order to deliver a uniformly quality-controlled surface ocean CO_2 database. The many researchers and funding agencies responsible for the collection of data and quality control are thanked for their contributions to SOCAT. The research leading to these results has received funding from the European Union's Horizon 2020 research and innovation program under the Marie Sklodowska-Curie grant agreement No 643052 744 (C-CASCADES project). NG acknowledges support by ETH Zürich. PL is supported by the Max Planck Society for the Advancement of Science.

Deleted: 5.

References

Ali, E.: The Inorganic Carbon Cycle in the Red Sea, Master's thesis, University of Bergen, 2008.

Anderson, L. G., Jutterström, S., Hjalmarsson, S., Wåhlström, I., and Semiletov, I. P.: Out-gassing of CO2 from Siberian Shelf seas by terrestrial organic matter decomposition, Geophys. Res. Lett., 36, L20601, doi:10.1029/2009GL040046, 2009.

Antonov, J. I., Seidov, D., Boyer, T. P., Locarnini, R. A., Mishonov, A. V., Garcia, H. E., Baranova, O. K., Zweng, M. M., and Johnson D. R.: in World Ocean Atlas 2009, Volume 2: Salinity, NOAA Atlas NESDIS, vol. 69, edited by S. Levitus, U.S. Gov. Print. Off., Washington, D. C., 2010.

Atlas, R., Hoffman, R.N., Ardizzone, J., Leidner, S.M., Jusem, J.C., Smith, D.K. and Gombos, D.: A cross-calibrated, multiplatform ocean surface wind velocity product for meteorological and oceanographic applications. Bulletin of the American Meteorological Society, 92(2), 157-174, 2011.

Bakker, D. C. E., Pfeil, B., Smith, K., Hankin, S., Olsen, A., Alin, S. R., Cosca, C., Harasawa, S., Kozyr, A., Nojiri, Y., O'Brien, K. M., Schuster, U., Telszewski, M., Tilbrook, B., Wada, C., Akl, J., Barbero, L., Bates, N. R., Boutin, J., Bozec, Y., Cai, W.-J., Castle, R. D., Chavez, F. P., Chen, L., Chierici, M., Currie, K., De Baar, H. J. W., Evans, W., Feely, R. A., Fransson, A., Gao, Z., Hales, B., Hardman-Mountford, N. J., Hoppema, M., Huang, W.-J., Hunt, C. W., Huss, B., Ichikawa, T., Johannessen, T., Jones, E. M., Jones, S., Jutterstrom, S., Kitidis, V., Körtzinger, A., Landschützer, P., Lauvset, S. K., Lefèvre, N., Manke, A. B., Mathis, J. T., Merlivat, L., Metzl, N., Murata, A., Newberger, T., Omar, A. M., Ono, T., Park, G.-H., Paterson, K., Pierrot, D., Ríos, A. F., Sabine, C. L., Saito, S., Salisbury, J.,

Deleted: 6.

1034 Sarma, V. V. S. S., Schlitzer, R., Sieger, R., Skjelvan, I., Steinhoff, T., Sullivan, K. F., Sun,
1035 H., Sutton, A. J., Suzuki, T., Sweeney, C., Takahashi, T., Tjiputra, J., Tsurushima, N., Van
1036 Heuven, S. M. A. C., Vandemark, D., Vlahos, P., Wallace, D. W. R., Wanninkhof, R.,
1037 Watson, A. J.: An update to the Surface Ocean CO2 Atlas (SOCAT version 2). Earth
1038 System Science Data 6: 69-90. doi:10.5194/essd-6-69-2014, 2014.
1039 Bakker, D. C. E. et al. (92 authors) : A multi-decade record of high-quality fCO2 data in
1040 version 3 of the Surface Ocean CO2 Atlas (SOCAT), Earth Syst. Sci. Data, 8, 383-413,
1041 doi:10.5194/essd-8-383-2016, 2016
1042 Bates, N. R., Moran, S. B., Hansell, D. A., and Mathis, J. T.: An increasing CO_2 sink in the
1043 Arctic Ocean due to sea-ice loss. Geophys. Res. Lett., 33(23), L23609, doi:
1044 10.1029/2006GL027028, 2006.
1045 Bates, N. R., and Mathis, J. T.: The Arctic Ocean marine carbon cycle: Evaluation of air-sea
1046 CO2 exchanges, ocean acidification impacts and potential feedbacks, Biogeosciences, 6,
1047 2433–2459, doi:10.5194/bg-6-2433-2009, 2009.
1048 Bauer, J. E., Cai, W.-J., Raymond, P. A., Bianchi, T. S., Hopkinson, C. S., and Regnier, P. A.
1049 G.: The changing carbon cycle of the coastal ocean, Nature, 504, 61–70,
1050 doi:10.1038/nature12857, 2013.
1051 Borges, A. V., Delille, B., and Frankignoulle, M.: Budgeting sinks and sources of CO2 in the
1052 coastal ocean: Diversity of ecosystems counts, Geophys. Res. Lett., 32, L14601,
1053 doi:10.1029/2005GL023053, 2005.
1054 Bourgeois, T., Orr, J. C., Resplandy, L., Terhaar, J., Ethé, C., Gehlen, M., and Bopp, L.:
1055 Coastal-ocean uptake of anthropogenic carbon, Biogeosciences, 13, 4167-4185,
1056 doi:10.5194/bg-13-4167-2016, 2016.

Deleted:

Cai, W. J.: Estuarine and coastal ocean carbon paradox: CO2 sinks or sites of terrestrial carbon incineration?, Annu. Rev. Mar. Sci., 3, 123–145, 2011.

Cavalieri, D. J., Parkinson, C. L., Gloersen, P., and Zwally, H.: Sea Ice Concentrations from Nimbus-7 SMMR and DMSP SSM/I-SSMIS Passive Microwave Data, years 1990–2011, NASA DAAC at the Natl. Snow and Ice Data Cent., Boulder, Colo. (Updated yearly.), 1996.

Chen, C.T.A., and Borges, A.V.: Reconciling opposing views on carbon cycling in the coastal ocean: continental shelves as sinks and near-shore ecosystems as sources of atmospheric CO2, Deep-Sea Research II, 56 (8-10), 578-590, 2009.

Chen, C. T. A., Huang, T. H., Chen, Y. C., Bai, Y., He, X., and Kang, Y.: Air-sea exchanges of CO2 in the world's coastal seas, Biogeosciences, 10, 6509–6544, doi:10.5194/bg-10-6509-2013, 2013.

Chen, S., Hu, C., Byrne, R. H., Robbins, L. L., and Yang, B.: Remote estimation of surface pCO2 on the West Florida Shelf, Continental Shelf Research, 128, 10–25, 2016.

Cooley, S. R., V. J. Coles, A. Subramaniam, and P. L. Yager (2007), Seasonal variations in the Amazon plume-related atmospheric carbon sink, Global Biogeochem. Cycles, 21, GB3014, doi:10.1029/2006GB002831.

Crossland, C. J., Kremer, H. H., Lindeboom, H. J., Marshall Crossland, J. I., and LeTissier, M. D. A. (Eds.): Coastal Fluxes in the Anthropocene, Global Change – The IGBP Series: 232 pp, Berlin, Heidelberg, Springer-Verlag, Germany, 2005.

Dee, D.P.: The ERA-Interim reanalysis: Configuration and performance of the data assimilation system. Q. J. R. Meteorol. Soc., 137, pp.553–597, 2010.

Dee, D. P., Uppala, S. M., Simmons, A. J., Berrisford, P., Poli, P., Kobayashi, S., Andrae, U.,

Balmaseda, M. A., Balsamo, G., Bauer, P., Bechtold, P., Beljaars, A. C. M., van de Berg, L., Bidlot, J., Bormann, N., Delsol, C., Dragani, R., Fuentes, M., Geer, A. J., Haimberger, L., Healy, S. B., Hersbach, H., Hòlm, E. V., Isaksen, L., Kallberg, P., Köhler, M., Matricardi, M., Mcnally, A. P., Monge-Sanz, B. M., Morcrette, J. J., Park, B. K., Peubey, C., de Rosnay, P., Tavolato, C., Thépaut, J. N. and Vitart, F.: The ERA-Interim reanalysis: Configuration and performance of the data assimilation system, Q. J. R. Meteorol. Soc., 137(656), 553–597, doi:10.1002/qj.828, 2011.

Doney, S. C.: The Growing Human Footprint on Coastal and Open-Ocean Biogeochemistry, Science 328(5985), 1210-1216, doi:10.1126/science.1185198, 2010.

Good, S. A., M. J. Martin and N. A. Rayner, 2013. EN4: quality controlled ocean temperature and salinity profiles and monthly objective analyses with uncertainty estimates, Journal of Geophysical Research: Oceans, 118, 6704-6716, doi:10.1002/2013JC009067

Gruber, N.: Ocean biogeochemistry: Carbon at the coastal interface, Nature, 517, 148–149, doi:10.1038/nature14082, 2015.

Grimm, R., Notz, D., Glud, R.N., Rysgaard, S. and Six, K.D.: Assessment of the sea-ice carbon pump: Insight from a three-dimensional ocean-sea-ice-biogeochemical model (MPIOM/HAMOCC). Elementa: Science of the Anthropocene, 4:000136, doi: 10.12952/journal.elementa.000136, 2016.

Ibánhez, J. S. P., D. Diverrès, M. Araujo, and N. Lefèvre (2015), Seasonal and interannual variability of sea-air CO2 fluxes in the tropical Atlantic affected by the Amazon River plume, Global Biogeochem. Cycles, 29, 1640–1655, doi:10.1002/2015GB005110.

Landschützer, P., Gruber, N., Bakker, D. C. E., Schuster, U., Nakaoka, S., Payne, M. R., Sasse, T., and Zeng, J.: A neural network-based estimate of the seasonal to inter-annual

variability of the Atlantic Ocean carbon sink, Biogeosciences, 10, 7793-7815, doi:10.5194/bg-10-7793-2013, 2013.

Landschützer, P., Gruber, N., Bakker, D. C. E., and Schuster, U.: Recent variability of the global ocean carbon sink, Global Biogeochemical Cycles, 28, 927–949, doi:10.1002/2014GB004853, 2014.

Landschützer, P., Gruber, N., Haumann, F. A. Rödenbeck, C. Bakker, D.C.E. , van Heuven, S. Hoppema, M., Metzl, N., Sweeney, C., Takahashi, T., Tilbrook, B. and Wanninkhof, R.: The reinvigoration of the Southern Ocean carbon sink, Science, 349, 1221-1224. doi: 10.1126/science.aab2620, 2015.

Landschützer, P., Gruber, N. Bakker, D.C.E.: Decadal variations and trends of the global ocean carbon sink, Global Biogeochemical Cycles, 30, doi:10.1002/2015GB005359, 2016

Laruelle, G. G., Dürr, H. H., Slomp, C. P., and Borges, A. V.: Evaluation of sinks and sources of CO_2 in the global coastal ocean using a spatially-explicit typology of estuaries and continental shelves, Geophys. Res. Lett., 37, L15607, doi: 10.1029/2010gl043691, 2010.

Laruelle, G. G., Dürr, H. H., Lauerwald, R., Hartmann, J., Slomp, C. P., Goossens, N., and Regnier, P. A. G.: Global multi-scale segmentation of continental and coastal waters from the watersheds to the continental margins, Hydrol. Earth Syst. Sci., 17, 2029–2051, doi:10.5194/hess-17-2029-2013, 2013.

Laruelle, G. G., Lauerwald, R., Pfeil, B., and Regnier, P.: Regionalized global budget of the CO2 exchange at the air-water interface in continental shelf seas, Global Biogeochemical Cycles, 28, 1199–1214, doi:10.1002/2014GB004832, 2014.

Laruelle, G. G., Lauerwald, R., Rotschi, J., Raymond, P. A., Hartmann, J., and Regnier, P.: Seasonal response of air–water CO2 exchange along the land–ocean aquatic continuum of

1127 the northeast North American coast., Biogeosciences, 12, 1447-1458,
1128 doi:10.5194/bg-12-1447-2015, 2015.
1129 Liu, K.-K., Atkinson, L., Quinones, R., and Talaue-McManus, L. (Eds.): Carbon and Nutrient
1130 Fluxes in Continental Margins, Global Change – The IGBP Series, 3, Springer-Verlag
1131 Berlin Heidelberg, 2010.
1132 Lohrenz, S. E., and Cai, W.-J.: Satellite ocean color assessment of air-sea fluxes of CO2 in a
1133 river-dominated coastal margin, Geophys. Res. Lett., 33, L01601,
1134 doi:10.1029/2005GL023942, 2006.
1135 Lovely, A., Loose, B., Schlosser, P., McGillis, W., Zappa C., Perovich, D., Brown, S., Morell,
1136 T., Hsueh, D., and Friedrich, R.: The Gas Transfer through Polar Sea ice experiment:
1137 Insights into the rates and pathways that determine geochemical fluxes. J. Geophys. Res.
1138 Ocean. 120:8177–8194, 2015.
1139 Locarnini, R. A., Mishonov, A. V., Antonov, J. I., Boyer, T. P., Garcia, H. E., Baranova, O. K.,
1140 Zweng, M. M., and Johnson D. R.: World Ocean Atlas 2009, Volume 1: Temperature,
1141 NOAA Atlas NESDIS, vol. 69, edited by S. Levitus, U.S. Gov. Print. Off., Washington, D.
1142 C., 2010.
1143 Moreau, S., Vancoppenolle, M., Bopp, L., Aumont, O., Madec, G., Delille, B., Tison, J.-L.,
1144 Barriat, P.-Y. and Goosse, H.: Assessment of the sea-ice carbon pump: Insights from a
1145 three-dimensional ocean-sea-ice-biogeochemical model (NEMO-LIM-PISCES). Elementa:
1146 Science of the Anthropocene, 4:000122, doi: 10.12952/journal.elementa.000122, 2016.
1147 Nakaoka, S., Telszewski, M., Nojiri, Y., Yasunaka, S., Miyazaki, C., Mukai, H., and Usui, N.:
1148 Estimating temporal and spatial variation of ocean surface pCO2 in the North Pacific
1149 using a self-organizing map neural network technique, Biogeosciences, 10, 6093-6106,

doi:10.5194/bg-10-6093-2013, 2013.

NASA Goddard Space Flight Center, Ocean Ecology Laboratory, Ocean Biology Processing Group; (Dataset Release 2016): MODIS-Aqua chlorophyll Data; NASA Goddard Space Flight Center, Ocean Ecology Laboratory, Ocean Biology Processing Group, 2016.

Omer, W. M. M.: Ocean acidification in the Arabian Sea and the Red Sea. Master's thesis, University of Bergen, 2011.

Parmentier, F.-J. W., Christensen, T. R., Sørensen, L. L., Rysgaard, S., McGuire, A. D., Miller, P. A., and Walker, D. A.: The impact of lower sea-ice extent on Arctic greenhouse-gas exchange, Nature Climate Change, 3, 195–202, doi:10.1038/nclimate1784, 2013.

Pfeil, B., Olsen, A., Bakker, D. C. E., Hankin, S., Koyuk, H., Kozyr, A., Malczyk, J., Manke, A., Metzl, N., Sabine, C. L., Akl, J., Alin, S. R., Bates, N., Bellerby, R. G. J., Borges, A., Boutin, J., Brown, P. J., Cai, W.-J., Chavez, F. P., Chen, A., Cosca, C., Fassbender, A. J., Feely, R. A., González-Dávila, M., Goyet, C., Hales, B., Hardman-Mountford, N., Heinze, C., Hood, M., Hoppema, M., Hunt, C. W., Hydes, D., Ishii, M., Johannessen, T., Jones, S. D., Key, R. M., Körtzinger, A., Landschützer, P., Lauvset, S. K., Lefèvre, N., Lenton, A., Lourantou, A., Merlivat, L., Midorikawa, T., Mintrop, L., Miyazaki, C., Murata, A., Nakadate, A., Nakano, Y., Nakaoka, S., Nojiri, Y., Omar, A. M., Padin, X. A., Park, G.-H., Paterson, K., Perez, F. F., Pierrot, D., Poisson, A., Ríos, A. F., Santana-Casiano, J. M., Salisbury, J., Sarma, V. V. S. S., Schlitzer, R., Schneider, B., Schuster, U., Sieger, R., Skjelvan, I., Steinhoff, T., Suzuki, T., Takahashi, T., Tedesco, K., Telszewski, M., Thomas, H., Tilbrook, B., Tjiputra, J., Vandemark, D., Veness, T., Wanninkhof, R., Watson, A. J., Weiss, R., Wong, C. S., and Yoshikawa-Inoue, H.: A uniform, quality controlled Surface Ocean CO2 Atlas (SOCAT), Earth System Science Data 5: 125-143.

doi:10.5194/essd-5-125-2013, 2013.

Regnier, P., Friedlingstein, P., Ciais, P., Mackenzie, F. T., Gruber, N., Janssens, I. A., Laruelle, G. G., Lauerwald, R., Luyssaert, S., Andersson, A. J., Arndt, S., Arnosti, C., Borges, A. V., Dale, A. W., Gallego-Sala, A., Goddéris, Y., Goossens, N., Hartmann, J., Heinze, C., Ilyina, T., Joos, F., LaRowe, D. E., Leifeld, J., Meysman, F. J. R., Munhoven, G., Raymond, P. A., Spahni, R., Suntharalingam, P. and Thullner, M.: Anthropogenic perturbation of the carbon fluxes from land to ocean. Nature Geoscience, 6, doi:10.1038/ngeo1830, 2013.

Rödenbeck, C., Bakker, D. C. E., Gruber, N., Iida, Y., Jacobson, A. R., Jones, S., Landschützer, P., Metzl, N., Nakaoka, S., Olsen, A., Park, G.-H., Peylin, P., Rodgers, K. B., Sasse, T. P., Schuster, U., Shutler, J. D., Valsala, V., Wanninkhof, R., and Zeng, J.: Data-based estimates of the ocean carbon sink variability – first results of the Surface Ocean pCO2 Mapping intercomparison (SOCOM), Biogeosciences, 12, 7251-7278, doi:10.5194/bg-12-7251-2015, 2015.

Sabine, C. L., et al. (76 authors): Surface Ocean CO2 Atlas (SOCAT) gridded data products, Earth System Science Data , 5, 145 153, doi:10.5194/essd-5-145-2013, 2013

Sasse, T. P., McNeil, B. I., and Abramowitz, G.: A new constraint on global air-sea CO_2 fluxes using bottle carbon data, Geophys. Res. Lett., 40, 1594–1599, doi:10.1002/grl.50342, 2013.

Sarma, V. V. S. S., Monthly variability in surface pCO2 and net air-sea CO2 flux in the Arabian Sea, J. Geophys. Res., 108 (C8), 3255, doi:10.1029/2001JC001062, 2003.

Shadwick, E. H., Thomas, H., Comeau, A., Craig, S. E., Hunt, C. W., and Salisbury, J. E.: Air-Sea CO2 fluxes on the Scotian Shelf: seasonal to multi-annual variability, Biogeosciences, 7, 3851–3867, doi:10.5194/bg-7-3851-2010, 2010.

1197 Signorini, S. R., Mannino, A., Najjar Jr., R. G., Friedrichs, M. A. M., Cai, W.-J., Salisbury, J.,
1198 Wang, Z. A., Thomas, H., and Shadwick, E.: Surface ocean pCO2 seasonality and sea-air
1199 CO2 flux estimates for the North American east coast, J. Geophys. Res.-Oceans, 118,
1200 5439–5460, doi:10.1002/jgrc.20369, 2013.
1201 Takahashi, T., Olafsson, J., Goddard, J. G., Chipman, D. W., and Sutherland, S. C.: Seasonal
1202 variation of CO2 and nutrients in the high-latitude surface oceans: A comparative study.
1203 Global Biogeochemical Cycles, 7(4), 843–878, 1993.
1204 Takahashi, T., Sutherland, S., and Kozyr A.: Global ocean surface water partial pressure of
1205 CO2 database: Measurements performed during 1957–2011 (Version 2011).
1206 ORNL/CDIAC-160, NDP-088(V2011), Carbon Dioxide Information Analysis Center,
1207 Oak Ridge Natl. Lab., U.S. Dep. of Energy, Oak Ridge, Tenn., 2012.
1208 Takahashi, T., Sutherland, S. C., and Kozyr, A.: Global Ocean Surface Water Partial Pressure
1209 of CO2 Database: Measurements Performed During 1957-2015 (Version 2015).
1210 ORNL/CDIAC-160, NDP-088(V2015). Carbon Dioxide Information Analysis Center,
1211 Oak Ridge National Laboratory, U.S. Department of Energy, Oak Ridge, Tennessee, doi:
1212 10.3334/CDIAC/OTG.NDP088(V2015), 2016.
1213 Thomas, H., and Schneider, B.: The seasonal cycle of carbon dioxide in Baltic Sea surface
1214 waters, J. Mar. Syst, 22, 53-67, 1999.
1215 Turi, G., Lachkar, Z., and Gruber, N.: Spatiotemporal variability and drivers of pCO2 and air–
1216 sea CO2 fluxes in the California Current System: an eddy-resolving modeling study,
1217 Biogeosciences, 11, 671-690, doi:10.5194/bg-11-671-2014, 2014.
1218 U.S. Department of Commerce, National Oceanic and Atmospheric Administration, National
1219 Geophysical Data Center. 2006. 2-minute Gridded Global Relief Data (ETOPO2v2).

http://www.ngdc.noaa.gov/mgg/fliers/06mgg01.html. Accessed 26 Dec 2008.

Vancoppenolle M., Meiners, K. M., Michel, C., Bopp, L., Brabant, F., Carnat, G., Delille, B., Lannuzel, D., Madec, G., Moreau, S., Tison, J.-L., and van der Merwe, P.: Role of sea ice in global biogeochemical cycles: Emerging views and challenges, Quaternary Science Reviews, 79, 207-230, doi:10.1016/j.quascirev.2013.04.011, 2013.

Wanninkhof, R., Park, G.-H., Takahashi, T., Sweeney, C., Feely, R., Nojiri, Y., Gruber, N., Doney, S. C., McKinley, G. A., Lenton, A., Le Quéré, C., Heinze, C., Schwinger, J., Graven, H., and Khatiwala, S.: Global ocean carbon uptake: magnitude, variability and trends, Biogeosciences, 10, 1983-2000, doi: 10.5194/bg-10-1983-2013, 2013.

Walsh, J. J.: On the nature of continental shelves, Academic Press, San Diego, New York, Berkeley, Boston, London, Sydney, Tokyo, Toronto, 1988.

Wijesekera, H. W., J. S. Allen, and P. A. Newberger, Modeling study of turbulent mixing over the continental shelf: Comparison of turbulent closure schemes, J. Geophys. Res., 108(C3), 3103, doi:10.1029/2001JC001234, 2003

Yasunaka, S., Murata, A., Watanabe, E., Chierici, M., Fransson, A., van Heuven, S., Hoppema, M., Ishii, M., Johannessen, T., Kosugi, N., Lauvset, S. K., Mathis, J. T., Nishino, S., Omar, A. M., Olsen, A., Sasano, D., Takahashi, T., and Wanninkhof, R.: Mapping of the air-sea CO2 flux in the Arctic Ocean and its adjacent seas: Basin-wide distribution and seasonal to interannual variability. Polar Science, 10(3):323-334, doi:10.1016/j.polar.2016.03.006, 2016.

Zeng, J., Nojiri, Y., Landschützer, P., Telszewski, M., and Nakaoka, S.: A global surface ocean fCO2 climatology based on a feed-forward neural network, J. Atmos. Ocean Technol., 31, 1838-1849, 2014.

1243

Table 1: Datasets used to create the environmental forcing files. The original spatial and temporal resolution and the main manipulations applied for their use in the SOM_FFN are also reported.

Predictor	dataset	resolution	reference	Manipulation
SST	EN4	0.25°, daily	Good et al., 2013	Monthly average
SSS	EN4	0.25°, daily	Good et al., 2013	Monthly average
Bathymetry	ETOPO2	2 minutes	US Department of Commerce, 2006	Aggregation to 0.25°
Sea ice	NSIDC	0.25°, monthly	Cavalieri et al., 1996	Monthly rate of change in sea ice coverage
Chlorophyll a	SeaWifs, MODIS	9km, monthly	NASA, 2016	Aggregation to 0.25°
Wind speed	ERA	0.25°, 6hours	Dee et al., 2011	Monthly average

Formatted: Justified

Table 2: List of the biogeochemical provinces, their geographic distribution and the environmental predictors used to calculate surface ocean pCO_2. SSS stands for sea surface salinity, SST for sea surface temperature, Bathy for bathymetry, Ice for sea-ice cover, Chl for chlorophyll concentration and Wind for wind speed.

Province	SSS	SST	Bathy	Ice	Chl	Wind
P1	X	X	X		X	X
P2	X	X	X		X	X
P3	X	X	X		X	X
P4	X	X	X		X	X
P5	X	X	X	X	X	X
P6	X	X	X	X	X	X
P7	X	X	X	X	X	X
P8	X	X	X	X		X
P9	X	X	X	X		X
P10	X	X	X	X		X

Deleted: 1

Formatted: Justified

Deleted: and

Deleted: X

Deleted: X

Deleted: X

Table 3: Root mean squared error between observed and calculated pCO_2 in the different biogeochemical provinces. The SOM-FFN results are compared to data extracted from the LDEO database (Takahashi et al, 2014) and the overlapping cells from the Landschützer et al. (2016) pCO_2 climatology.

	Surface	Ice Cover	SOCAT*		Landschützer	2016	LDEO	
Province	**Area (km^2)**	**(%)**	**Bias (µatm)**	**RMSE (µatm)**	**Bias (µatm)**	**RMSE (µatm)**	**Bias (µatm)**	**RMSE (µatm)**
P1	8.2 10^6	0	0.0	19.1	2.0	27.2	2.0	20.5
P2	10.9 10^6	0	0.2	24.7	9.3	24.2	1.3	27.2
P3	4.4 10^6	0	-0.3	16.1	2.2	37.9	2.3	22.7
P4	16.6 10^6	0	-0.2	31.2	8.0	21.1	-1.6	33.0
P5	7.5 10^6	57.1	0.0	34.2	11.5	30.9	-1.4	38.0
P6	4.8 10^6	0	0.0	24.3	6.8	18.1	1.3	27.9
P7	9.3 10^6	0.0	0.1	37.2	0.7	23.5	-0.2	52.5
P8	3.3 10^6	38.5	0.2	46.8	13.9	70.1	3.9	51.4
P9	2.9 10^6	54.3	-0.1	23.0	-5.2	42.5	-2.5	33.4
P10	9.0 10^6	45.8	0.0	35.7	-9.7	50.9	1.6	53.1
	76.9 10^6		0.0	32.9	3.9	34.7	0.0	39.2

Deleted: 2
Deleted: v3.0
Deleted: 15.5
Deleted: -5.4
Deleted: 27.8
Deleted: 8.6
Deleted: 26…7.2.5
Deleted: -0.4
Deleted: 29.3
Deleted: 6
Deleted: 1.6
Deleted: 17.9
Deleted: 5.4
Deleted: 5
Deleted: -0.2
Deleted: 4.1
Deleted: 7
Deleted: 1.8
Deleted: 25.7
Deleted: 3.1
Deleted: 23.6
Deleted: -
Deleted: 43.7
Deleted: 8…6.1
Deleted: 8
Deleted: 15.4
Deleted: 0.2
Deleted: 28.5

Table 4: Biases and root mean squared error (RMSE) between observed and calculated pCO_2 using only SST, SSS and bathymetry (STB) or SST, SSS, bathymetry and chlorophyll (STBC) as predictors.

Province	SOCAT* Bias (µatm)		SOCAT* RMSE (µatm)		LDEO* Bias (µatm)		LDEO* RMSE (µatm)	
	STB	STBC	STB	STBC	STB	STBC	STB	STBC
P1	0.0	-0.2	20.8	21.0	2.4	2.0	21.7	21.5
P2	-0.1	0.1	26.9	27.8	0.5	0.8	29.0	29.6
P3	0.0	-0.5	22.7	21.3	3.0	2.3	27.1	26.8
P4	0.0	-0.2	33.0	33.0	-1.7	-2.3	33.8	33.8
P5	0.2	0.1	52.7	42.2	-1.7	-0.9	56.9	44.5
P6	0.0	0.1	26.8	26.5	-0.5	0.6	28.9	28.0
P7	0.4	0.3	44.3	44.1	1.2	0.3	59.3	58.8
P8	0.1	0.4	82.6	80.0	9.1	9.0	56.3	58.5
P9	0.1	0.9	34.7	36.5	-2.6	-2.8	39.8	41.8
P10	-0.3	0.7	49.8	49.5	-3.9	-3.0	76.5	75.4
Global	0.1	0.2	43.9	42.4	0.0	0.0	48.0	45.0

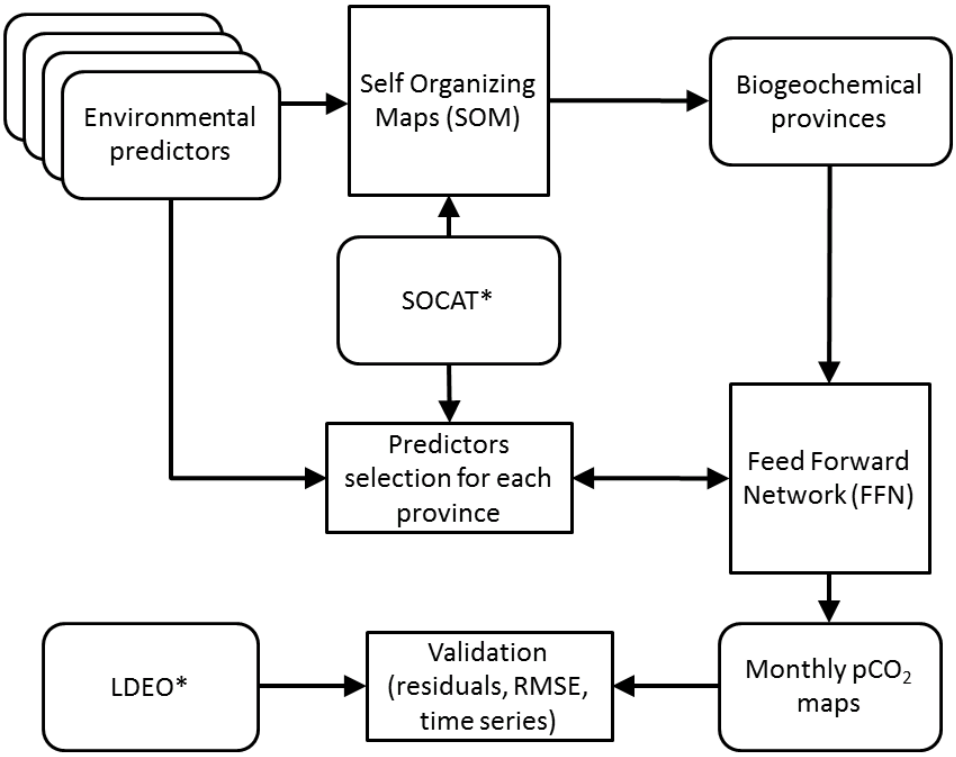

Figure 1: Schematic scheme of the different steps involved in the SOM-FFN artificial neural network calculations leading to continuous monthly pCO_2 maps over the 1998-2015 period.

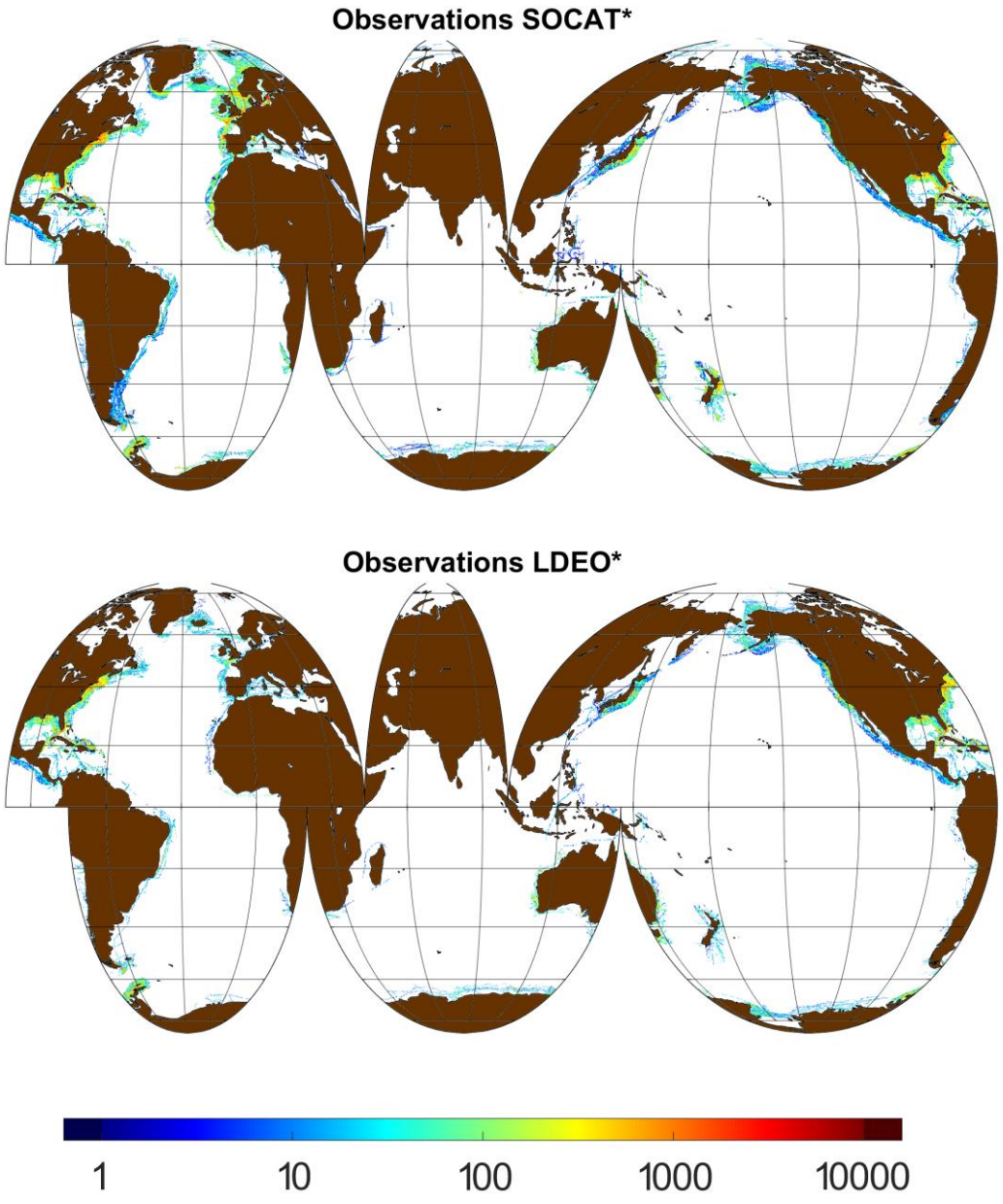

Figure 2: Number of observations contained in each 0.25° grid cell of the SOCAT* (top) and LDEO* (bottom) databases.

Formatted: Font: 12 pt

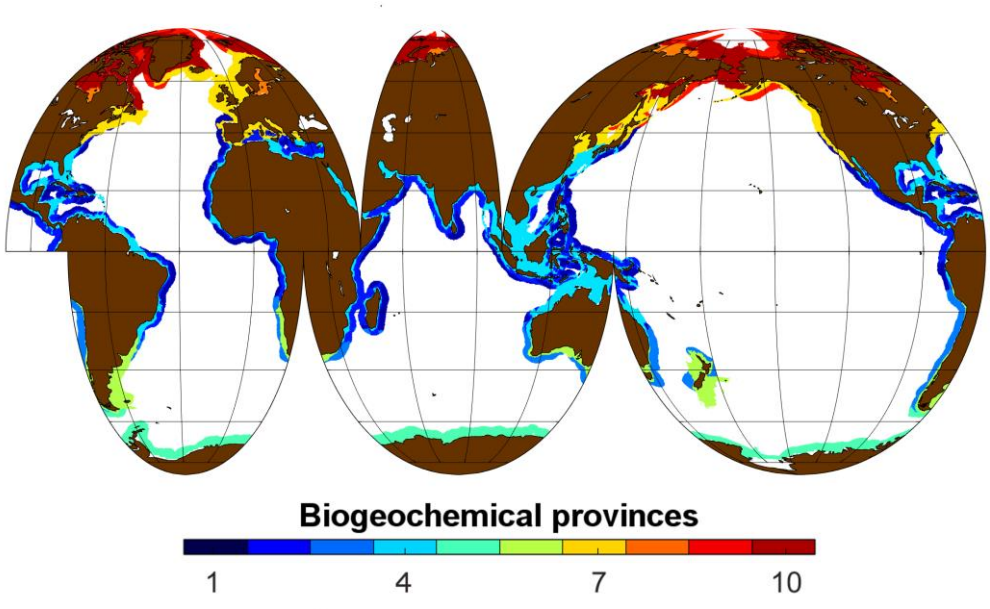

Figure 3: Map of the 10 different biogeochemical provinces generated by the artificial neural network method SOM-FFN.

Deleted:

Formatted: Font: 12 pt

Deleted: 1

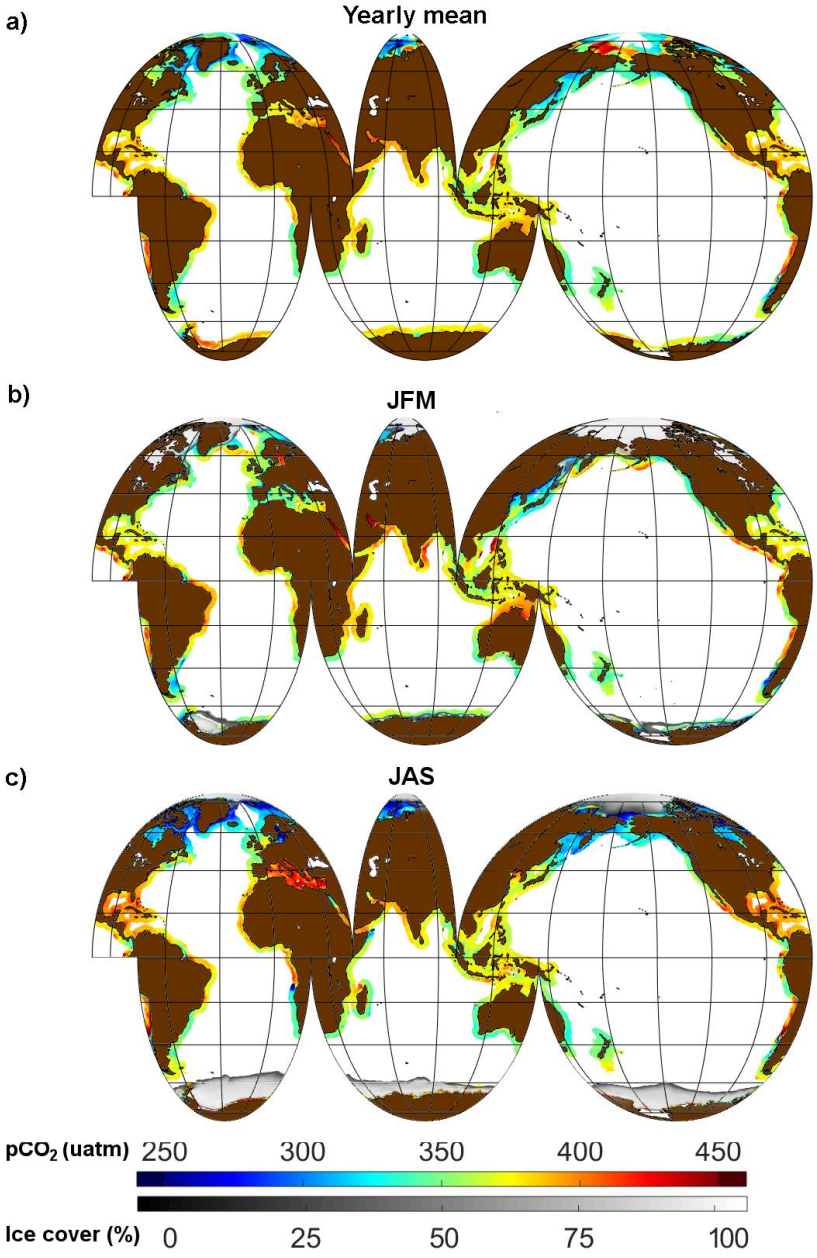

Figure 4: Climatological mean pCO_2 for (a) the long-term averaged pCO_2 (rainbow color scale) and sea-ice coverage (black-white color scale). The long-term average pCO_2 corresponds to roughly the nominal year 2006, as the average was formed over the full analysis period from 1998 through 2015; (b) the months of January, February and March; and (c) the months of July, August and September.

Deleted:

Formatted: Font: 12 pt

Deleted: 2

Deleted: 2014

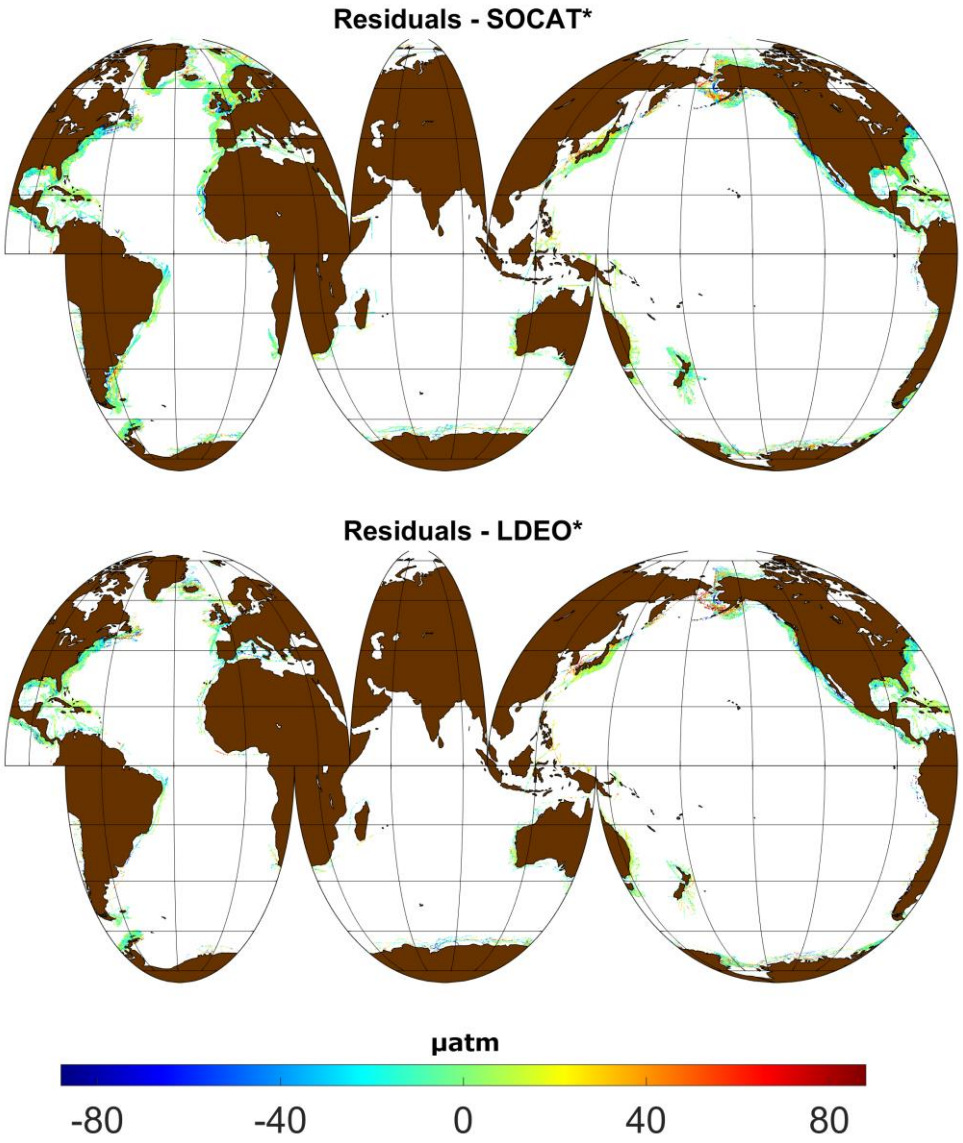

Figure 5: Mean residuals calculated as the difference between the SOM FFM pCO_2 outputs and pCO_2 observations from SOCAT* (top) and LDEO* (bottom).

Formatted: Font: 12 pt
Formatted: Justified
Formatted: Subscript
Formatted: Subscript
Formatted: Justified, Line spacing: 1,5 lines, Widow/Orphan control

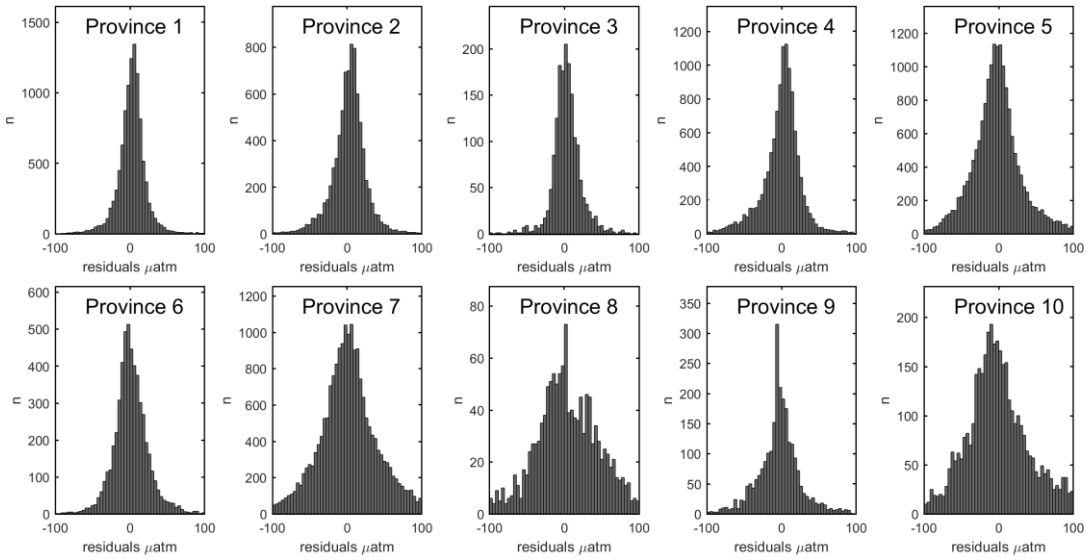

Figure 6: Histograms reporting the distribution of residuals between observed (LDEO*) and computed (SOM_FFN) pCO_2 in each biogeochemical province.

Formatted: Font: 12 pt

Formatted: Subscript

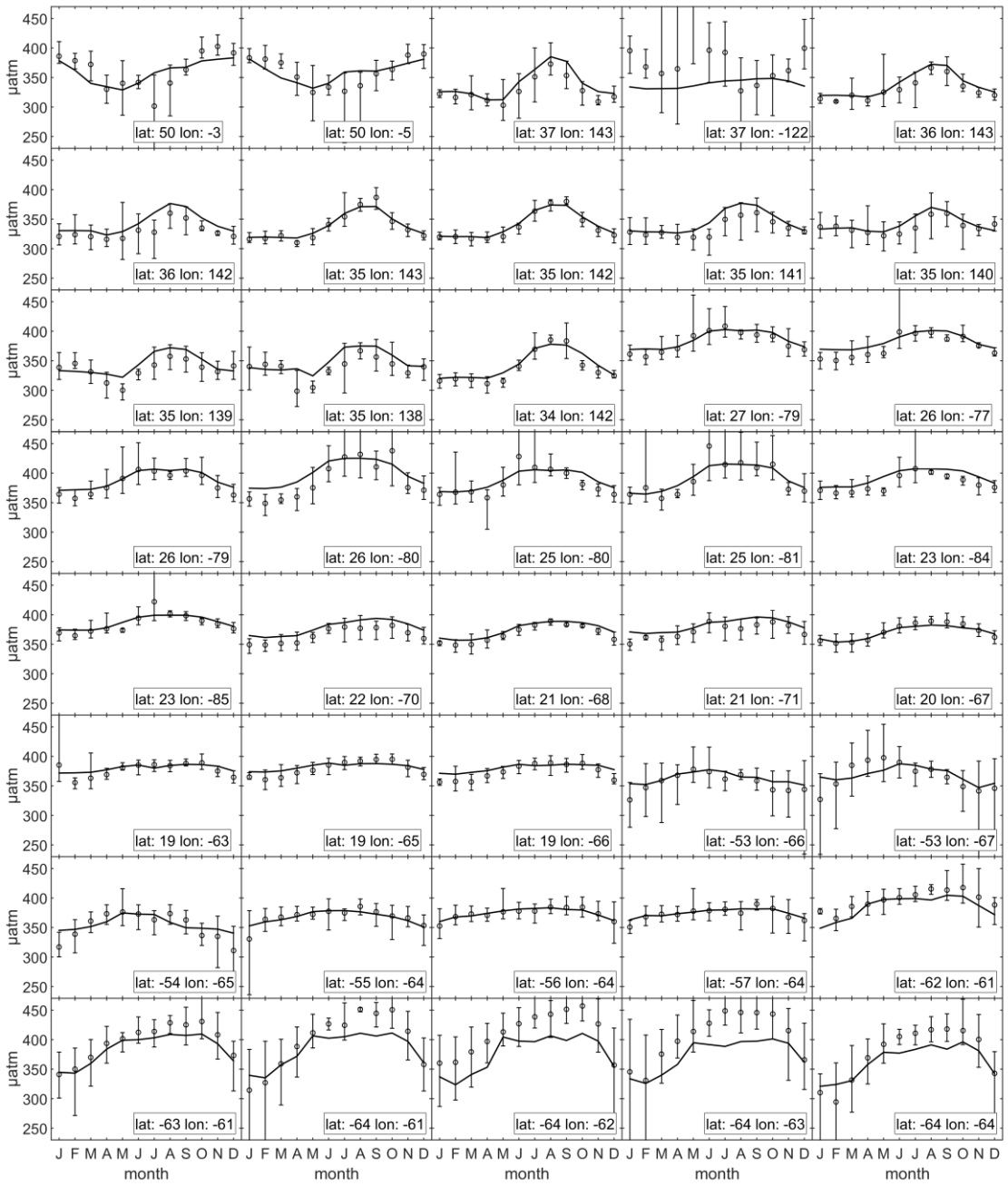

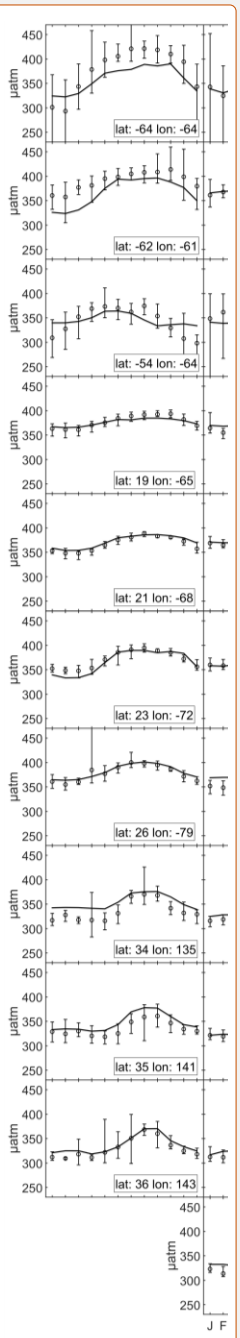

Figure 7: Climatological monthly mean pCO_2 extracted from the LDEO* database (points) and generated by the artificial neural network (lines) for grid cells having more than 40 months of data. The error bars associated with the data represent the inter-annual variability, reported as the highest and lowest recorded values for a given month at a given location.

Deleted:

Formatted: Font: 12 pt

Deleted: 3

Deleted: v2014

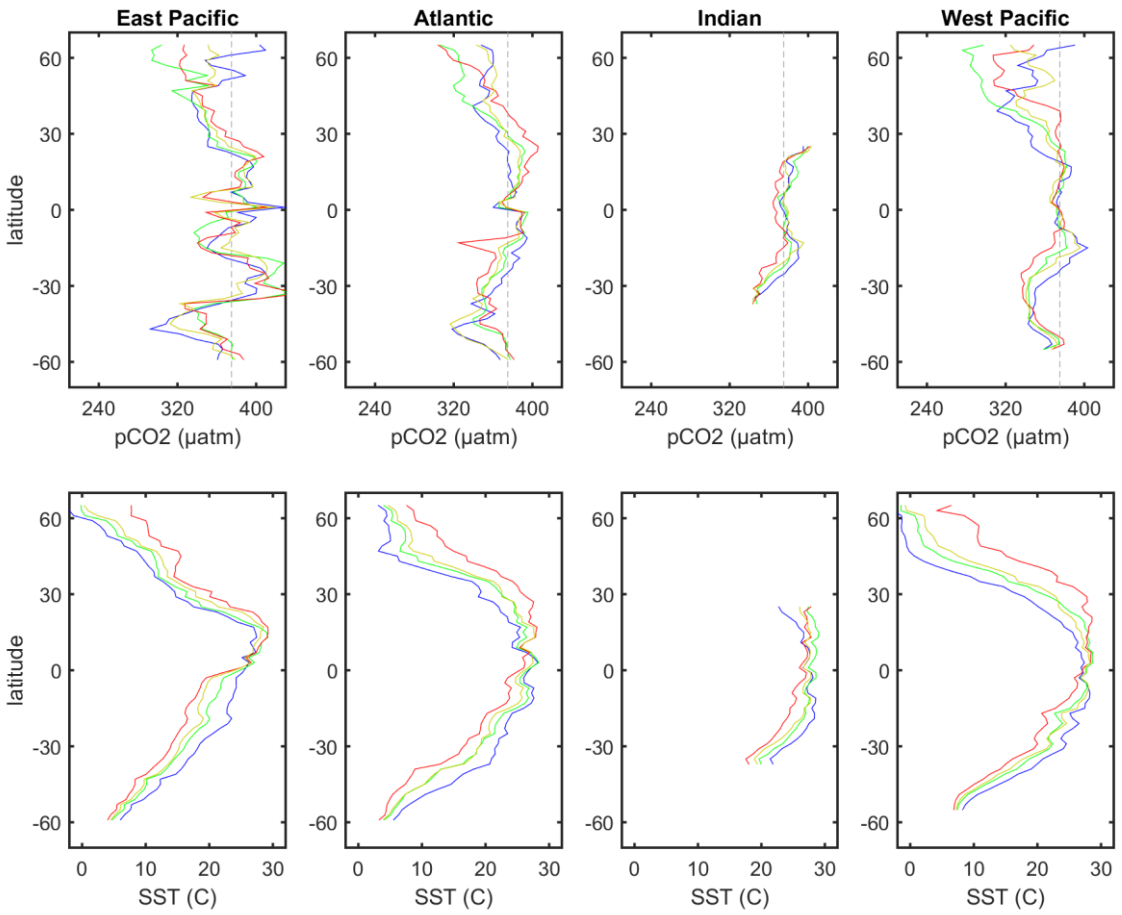

Figure 8: Seasonal-mean latitudinal profiles of pCO_2 (top) and SST (bottom) for the continental shelves surrounding 4 oceanic basins. Blue lines: averages over the months of January, February and March; green lines: averages over the months of April, May and June; red lines: averages over the months of July, August and September; yellow lines: averages over the months of October, November and December. The dashed line in the top panels represents the average atmospheric pCO_2 for year 2006.

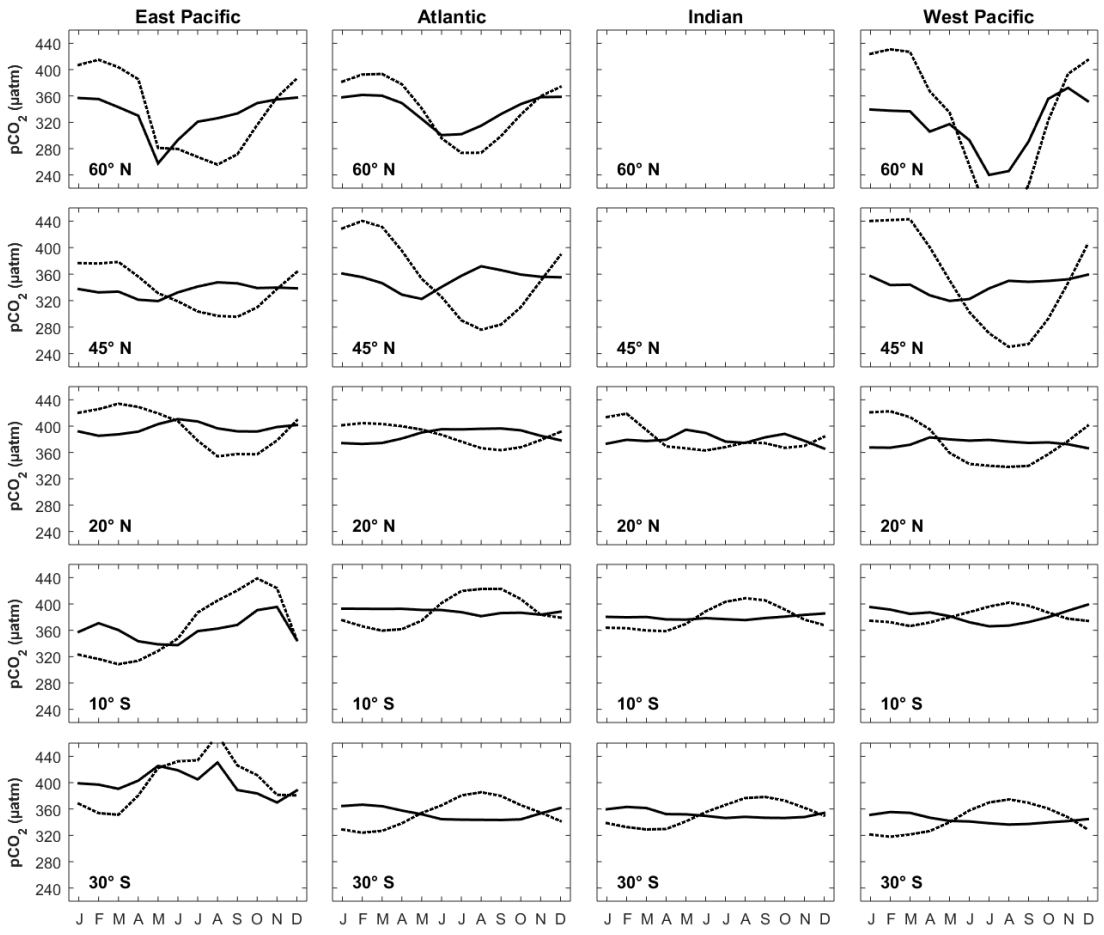

Figure 9: Seasonal cycle of observed (continuous lines) and temperature normalized pCO_2 ($pCO_{2(SSTmean)}$ dashed lines) at 5 different latitudes in 4 oceanic basins.

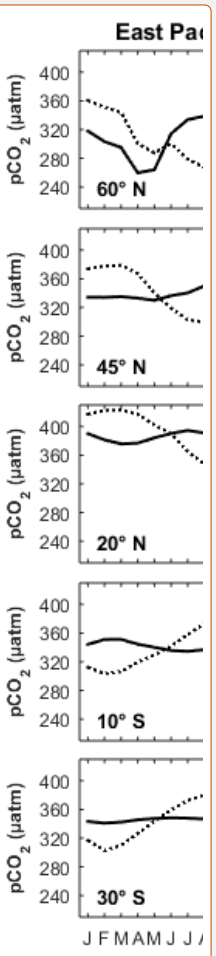

Deleted:

Formatted: Font: 12 pt

Deleted: 5

Formatted: Subscript